Supporting Information

For

DBU-catalyzed One-pot Synthesis of Nearly Any Metal Salt of Fatty Acid (M-FA): A Library of Metal Precursors to Semiconductor Nanocrystal Synthesis

*Siddhant Basel, Karishma Bhardwaj, Sajan Pradhan, Anand Pariyar and Sudarsan Tamang**

Department of Chemistry, School of Physical Sciences, Sikkim University, Tadong 737102, Sikkim, India

Sl.No.	Contents	Pg. No.
1.	TGA of indium stearate	S2
2.	^{1}H and ^{13}C NMR spectrum of indium stearate	S3
3.	^{1}H NMR spectrum of indium stearate with internal standard	S4
4.	FTIR spectra and TGA thermogram of the products	S5-S14

5.	^{1}H and ^{13}C NMR spectra of the products	S15-S28
6.	Photographs of colloidal dispersion of prepared semiconductor nanocrystals in hexane.	S28
7.	Characterization of $CsPbBr_3$ NCs as a representative example	S29

Table of contents

1. **TGA of indium stearate:**

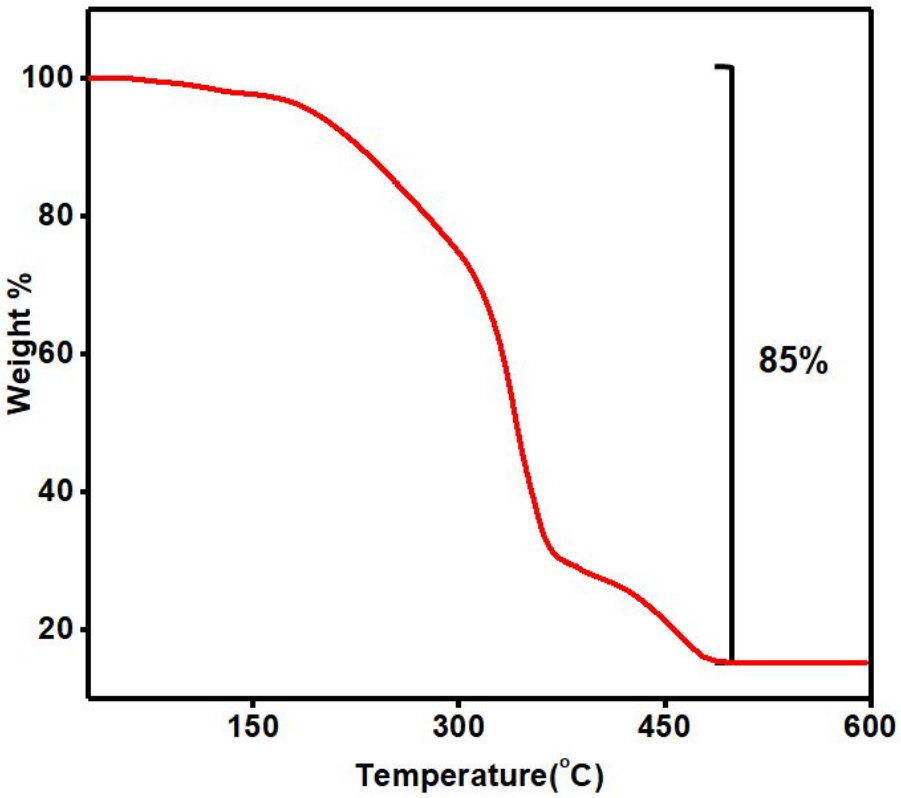

Figure S1: TGA plot of indium stearate (**3a**) showing a weight loss of 85% which corresponds to three stearates.

2. **^{1}H and ^{13}C NMR study of indium(III) stearate:**

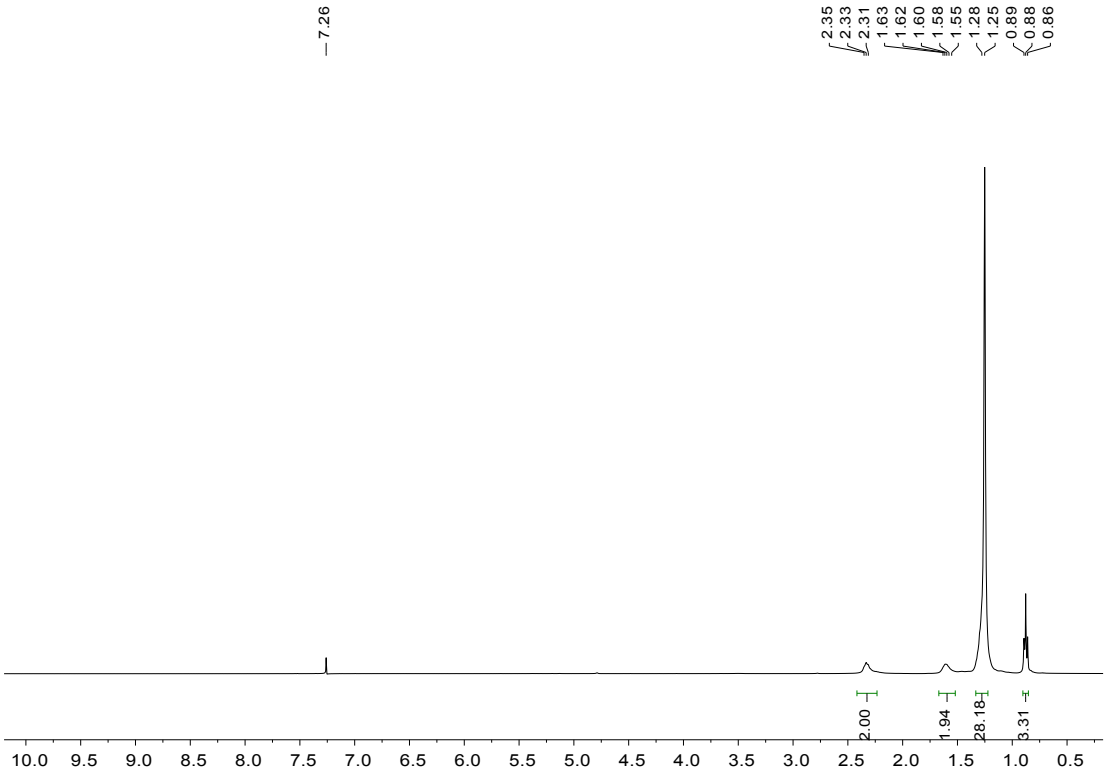

Figure S2: ^{1}H NMR spectrum of indium stearate **(3a)** (400 MHz, $CDCl_3$)

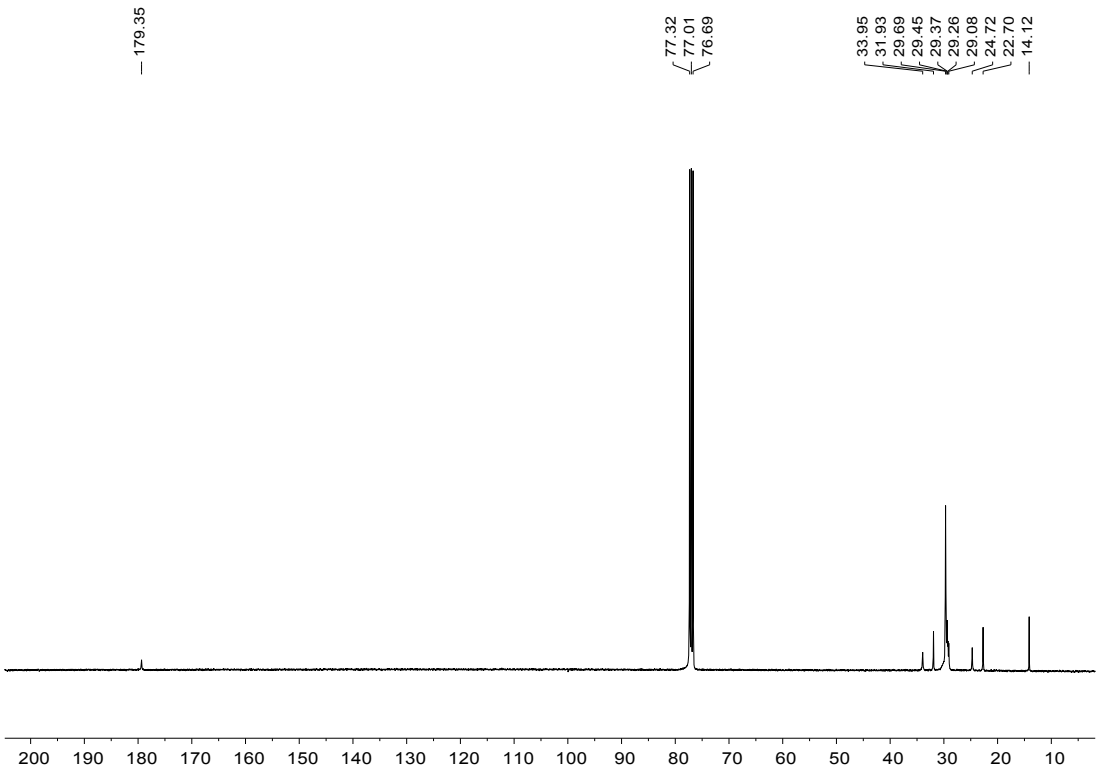

Figure S3: ^{13}C NMR spectrum of indium stearate **(3a)** (100 MHz, $CDCl_3$)

3. **^{1}H NMR of indium stearate with internal standard:**

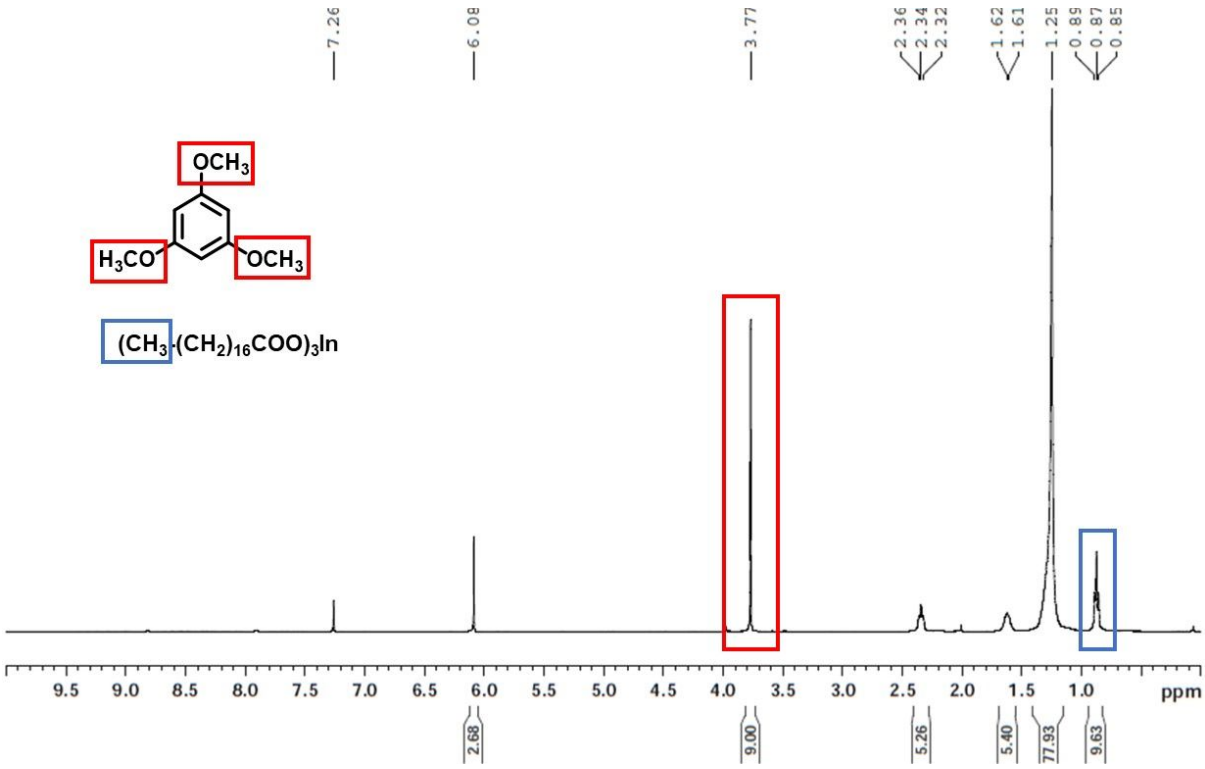

Figure S4: Detection of three stearate groups present in as-synthesized indium stearate (1 mmol) in ^{1}H NMR using internal standard 1,3,5-trimethoxybenzene (1 mmol).

4. FTIR spectra and TGA thermograms:

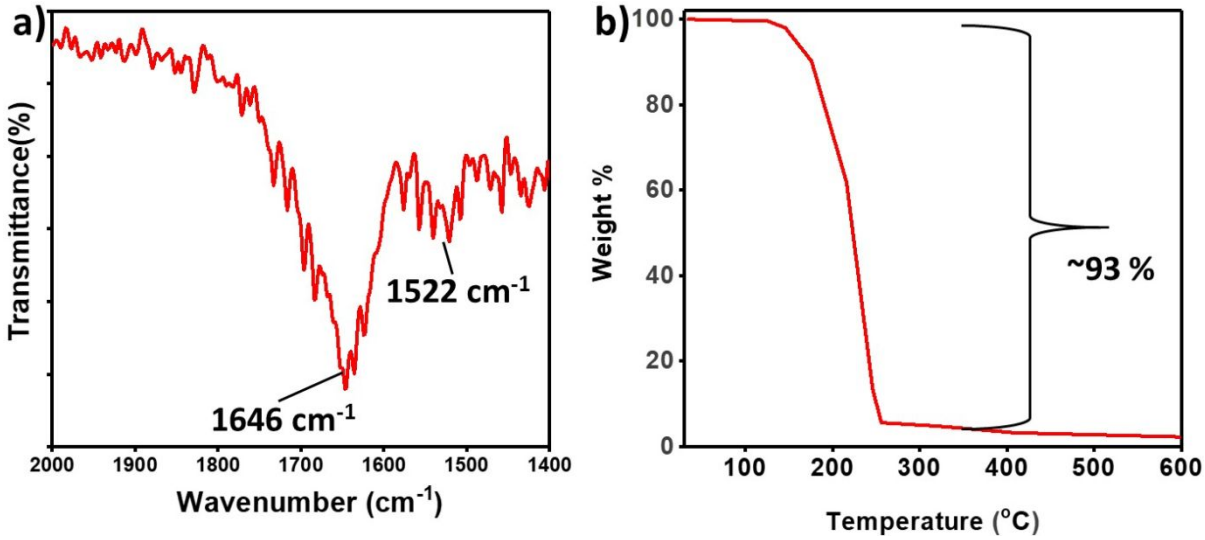

Figure S5: a) FTIR spectrum of gallium stearate (**3b**) showing characteristic -COO$^-$ asymmetric stretching at 1646 cm^{-1} and 1522 cm^{-1}. b) TGA thermogram of gallium stearate (**3b)** showing ~93 % loss of weight in the temperature range 130-260 ^{o}C corresponding to three stearates.

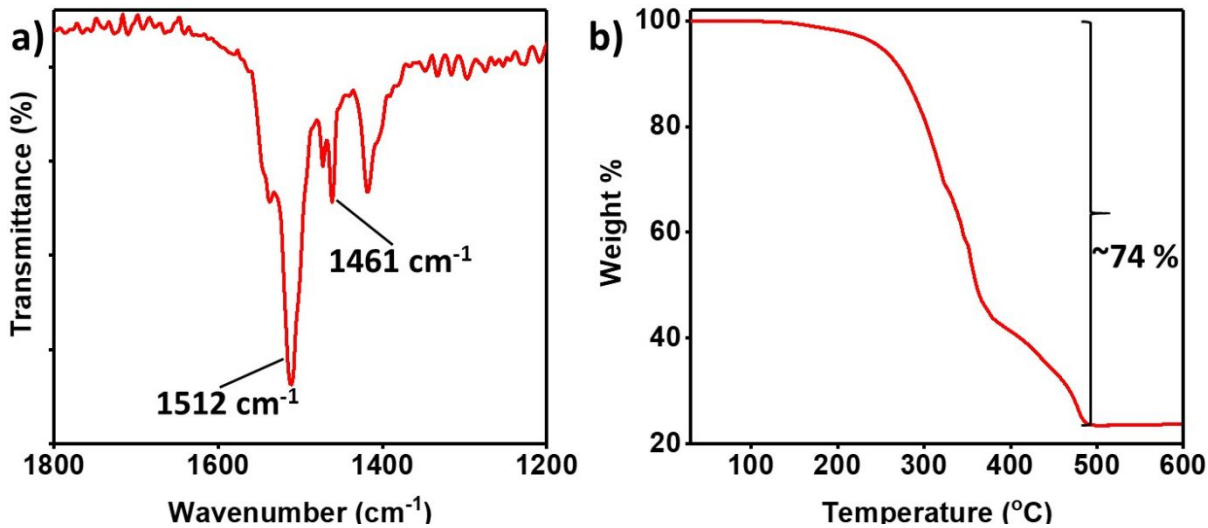

Figure S6: a) FTIR spectrum of lead stearate (**3c**) depicting asymmetric -COO$^-$ asymmetric stretching at 1512 cm^{-1} and symmetric stretching at 1461 cm^{-1}. b) TGA thermogram of lead stearate (**3c)** displaying ~74 % loss of weight in temperature range 210-490 ^{o}C corresponding to two stearates.

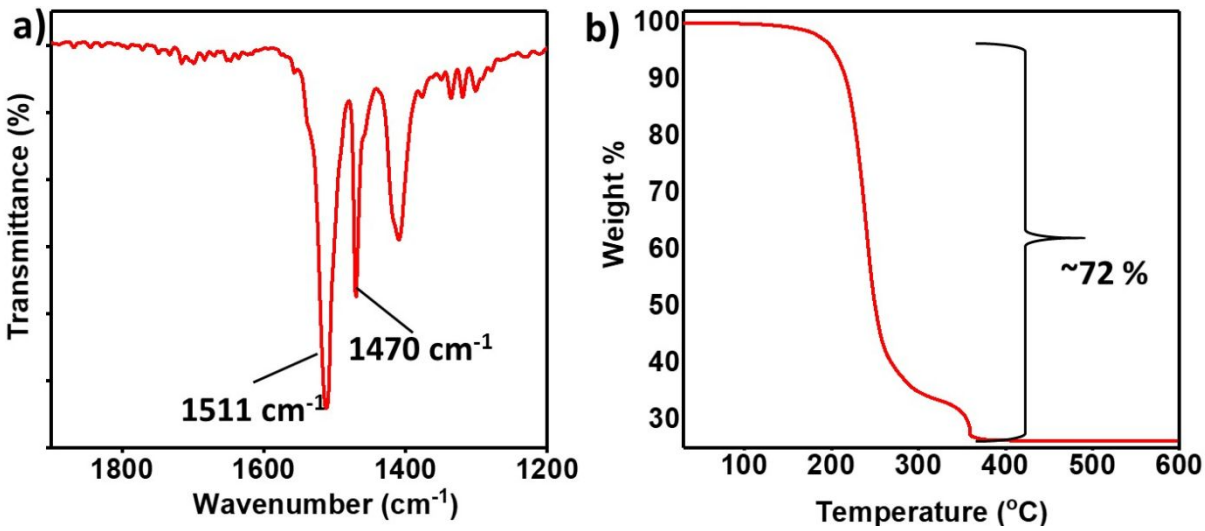

Figure S7: a) FTIR spectrum of silver stearate (**3d**) showing characteristic -COO$^-$ asymmetric stretching at 1511 cm^{-1} and symmetric stretching at 1470 cm^{-1}. b) TGA thermogram of silver stearate (**3d)** displaying ~72 % loss of weight in temperature range 180-360 ^{o}C consistent with one stearate.

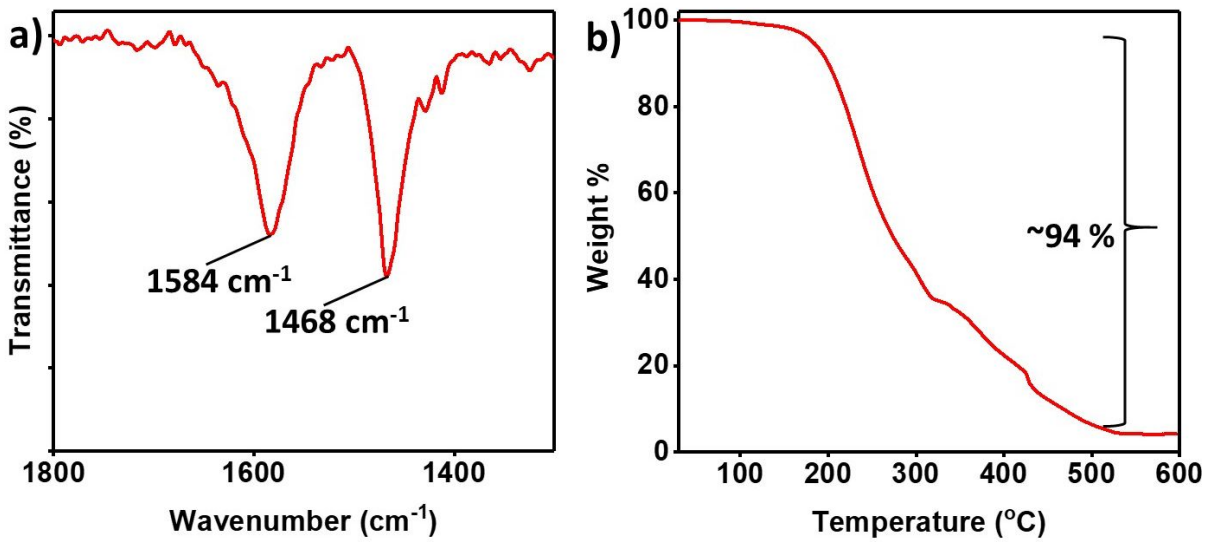

Figure S8: a) FTIR spectrum of aluminum stearate (**3e**) showing characteristic -COO$^-$ asymmetric stretching at 1584 cm^{-1} and symmetric stretching at 1468 cm^{-1}. b) TGA thermogram of aluminum stearate (**3e)** showing ~94 % loss of weight in temperature range 170-530 ^{o}C corresponding to three stearates.

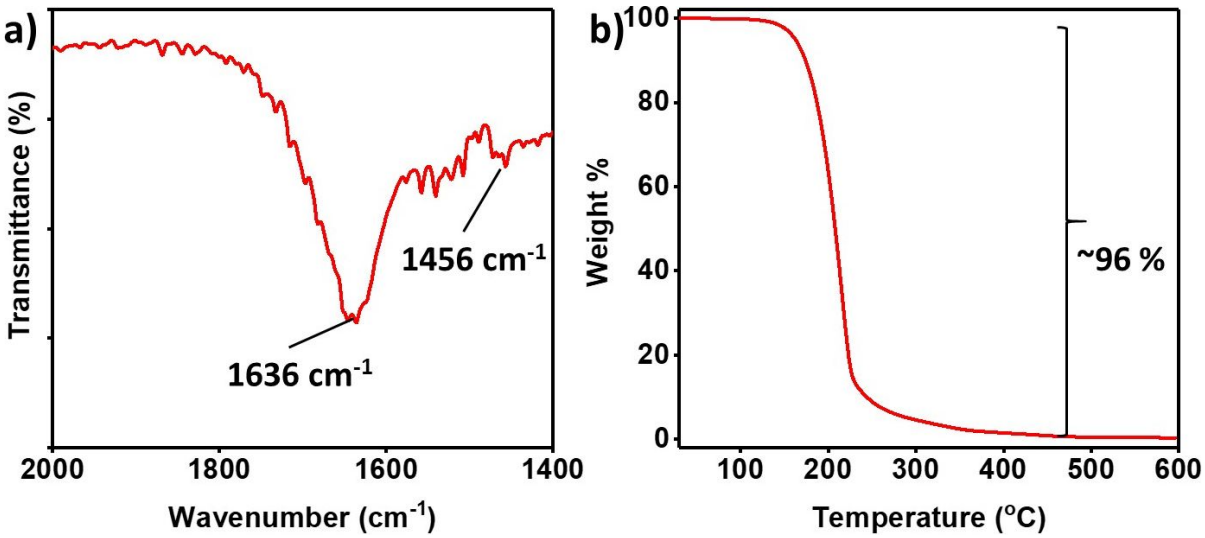

Figure S9: a) FTIR spectrum of ferric stearate (**3f**) showing characteristic -COO$^-$ asymmetric stretching at 1636 cm^{-1} and symmetric stretching at 1456 cm^{-1}. b) TGA thermogram of ferric stearate (**3f)** displaying ~96 % loss of weight in temperature range 140-360 ^{o}C consistent with three stearates.

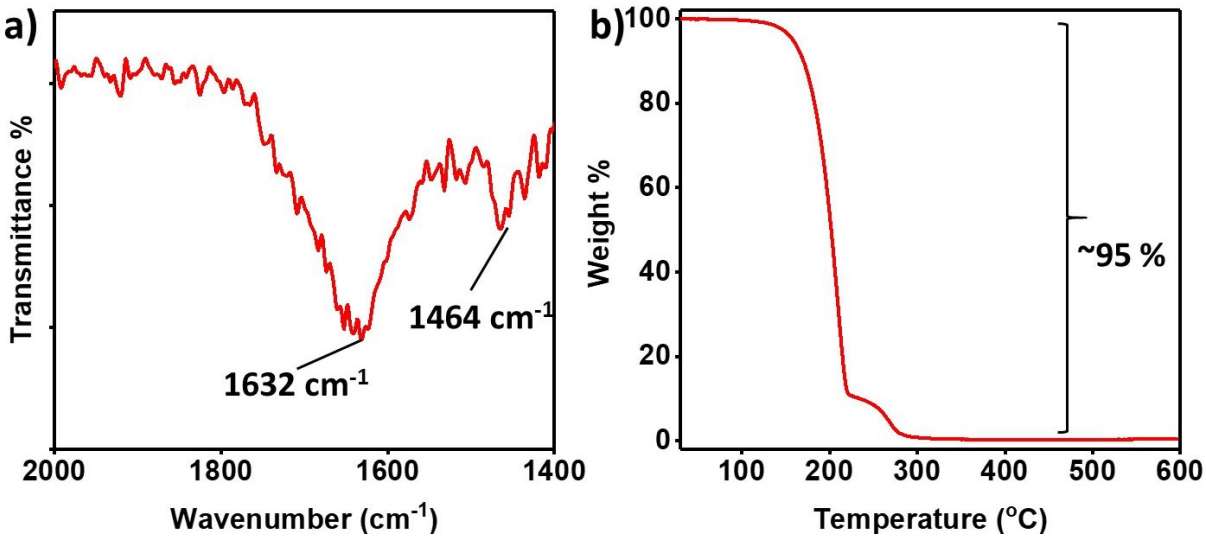

Figure S10: a) FTIR spectrum of copper stearate (**3g**) showing characteristic -COO$^-$ asymmetric stretching at 1632 cm^{-1} and symmetric stretching at 1464 cm^{-1}. b) TGA thermogram of copper stearate (**3g)** showing ~95 % loss of weight in temperature range 140-290 ^{o}C corresponding to two stearates.

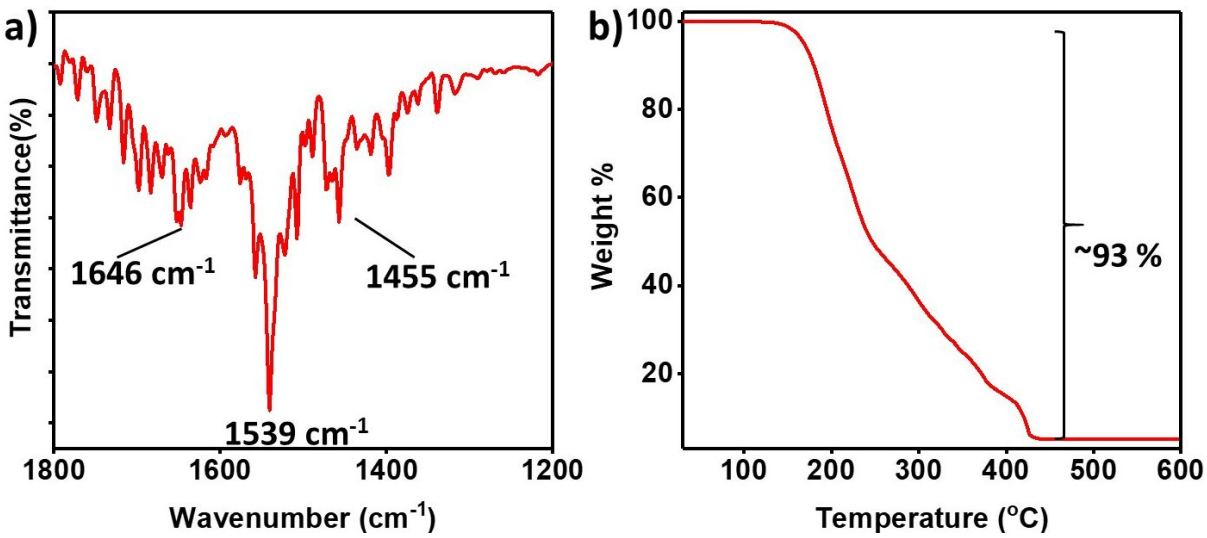

Figure S11: a) FTIR spectrum of cobalt stearate (**3h**) showing characteristic -COO$^-$ asymmetric stretching at 1646 cm^{-1} and 1539 cm^{-1} and symmetric stretching at 1455 cm^{-1}. b) TGA thermogram of cobalt stearate (**3h)** displaying ~93 % loss of weight in temperature range 145-430 ^{o}C consistent with two stearates.

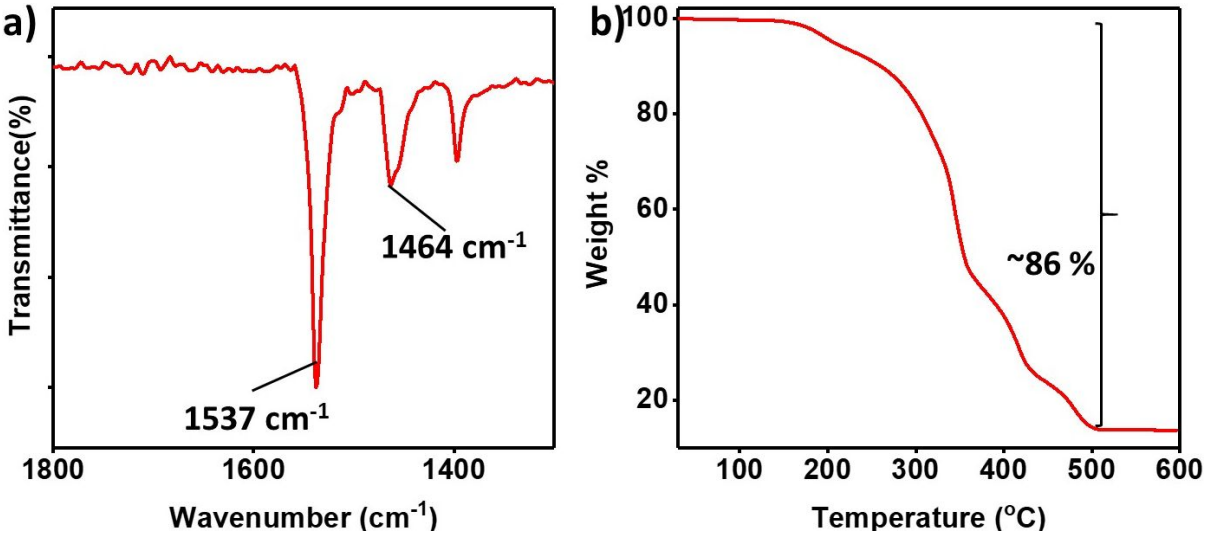

Figure S12: a) FTIR spectrum of zinc stearate (**3i**) showing characteristic -COO$^-$ asymmetric stretching at 1537 cm^{-1} and symmetric stretching at 1464 cm^{-1}. b) TGA thermogram of zinc stearate (**3i)** showing ~86 % loss of weight in the temperature range 170-500 ^{o}C corresponding to two stearates.

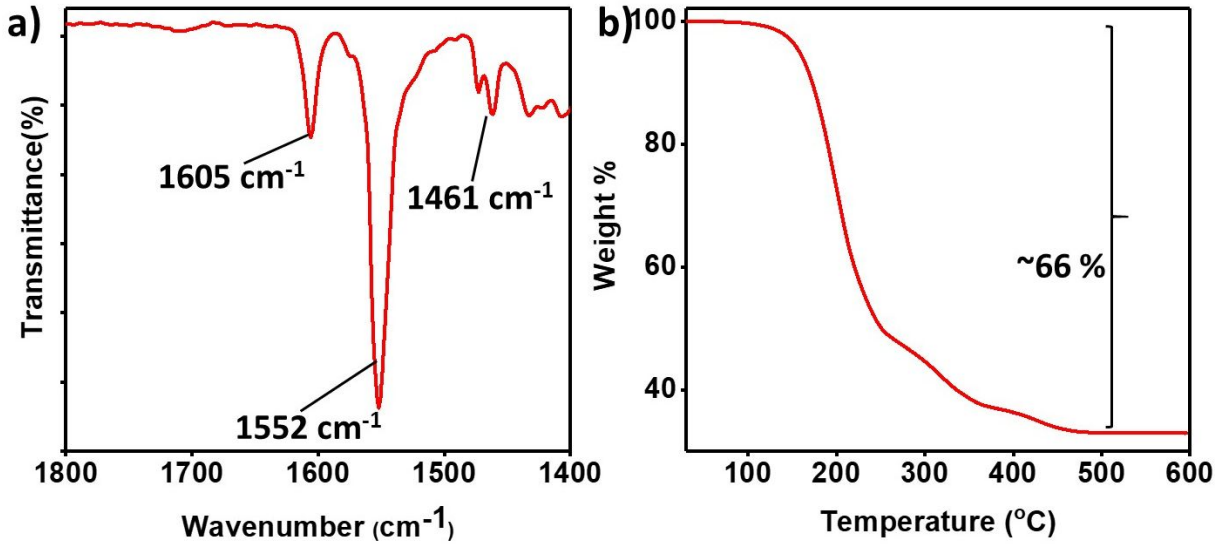

Figure S13: a) FTIR spectrum of tin stearate (**3j**) depicting characteristic -COO$^-$ asymmetric stretching at 1605 cm^{-1} and 1552 cm^{-1} and symmetric stretching at 1461 cm^{-1}. b) TGA thermogram of tin stearate (**3j)** displaying ~66 % loss of weight in the temperature range 130-470 ^{o}C corresponding to two stearates.

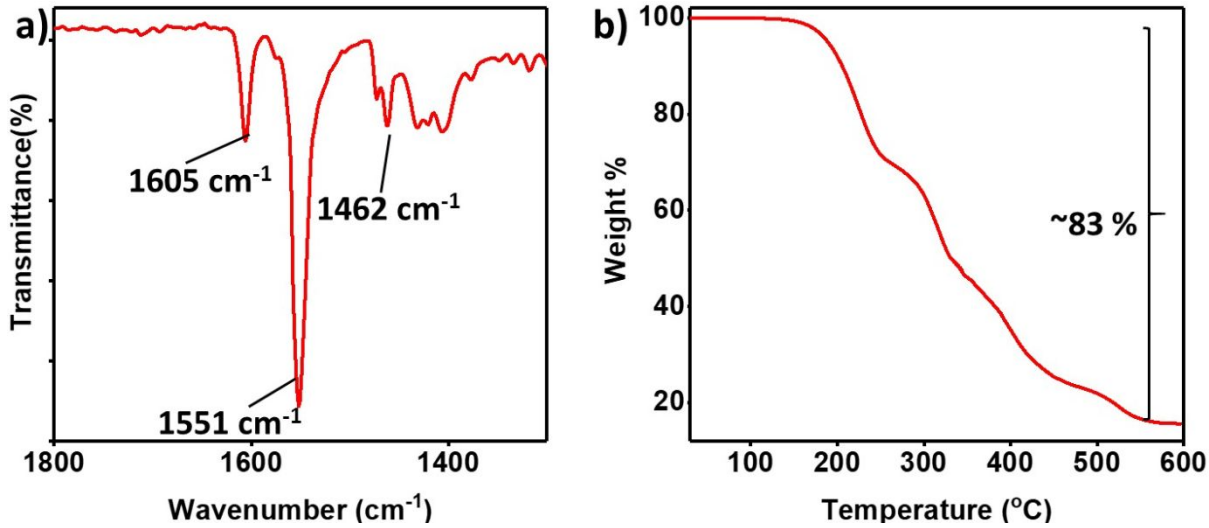

Figure S14: a) FTIR spectrum of cadmium stearate (**3k**) showing characteristic -COO$^-$ asymmetric stretching at 1605 cm^{-1} and 1551 cm^{-1} and symmetric stretching at 1462 cm^{-1}. b) TGA thermogram of cadmium stearate (**3k)** showing ~83 % loss of weight in the temperature range 160-570 ^{o}C corresponding to two stearates.

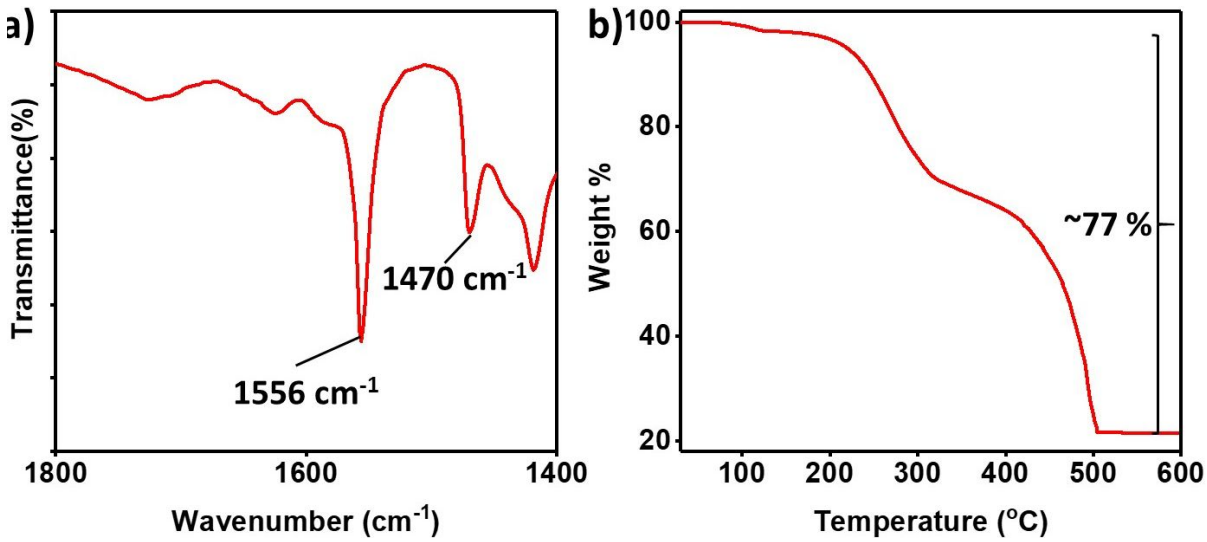

Figure S15: a) FTIR spectrum of potassium stearate (**3l**) depicting characteristic -COO$^-$ asymmetric stretching at 1556 cm^{-1} and symmetric stretching at 1470 cm^{-1}. b) TGA thermogram of potassium stearate (**3l)** showing ~77 % loss of weight in the temperature range 220-510 ^{o}C corresponding to one stearate.

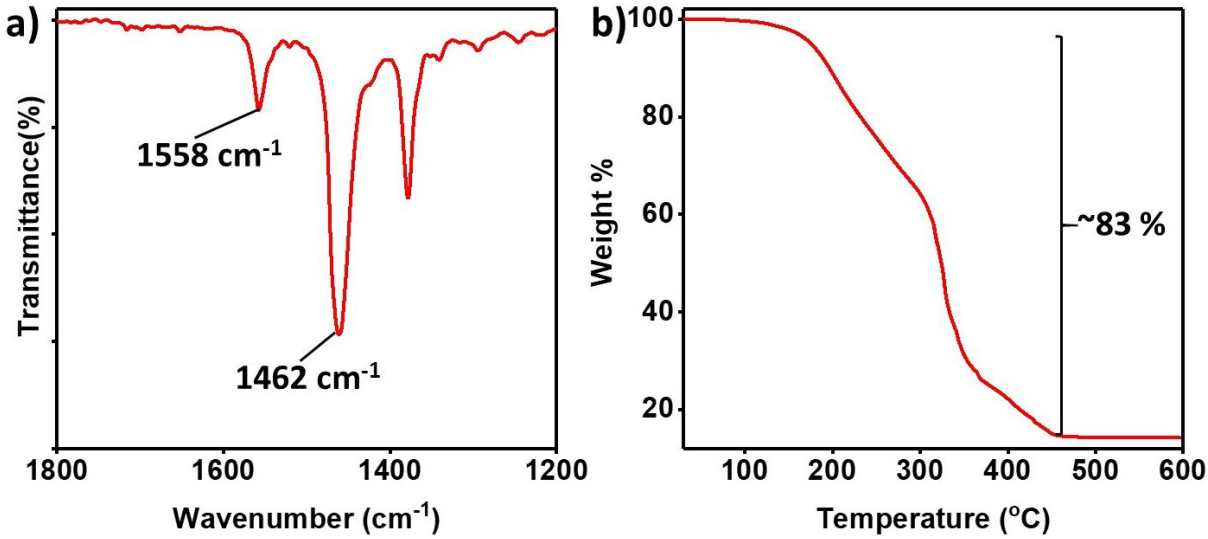

Figure S16: a) FTIR spectrum of indium myristate (**3m**) showing characteristic -COO$^-$ asymmetric stretching at 1558 cm^{-1} and symmetric stretching at 1462 cm^{-1}. b) TGA thermogram of indium myristate (**3m)** displaying ~83 % loss of weight in the temperature range 160-450 ^{o}C corresponding to three myristates.

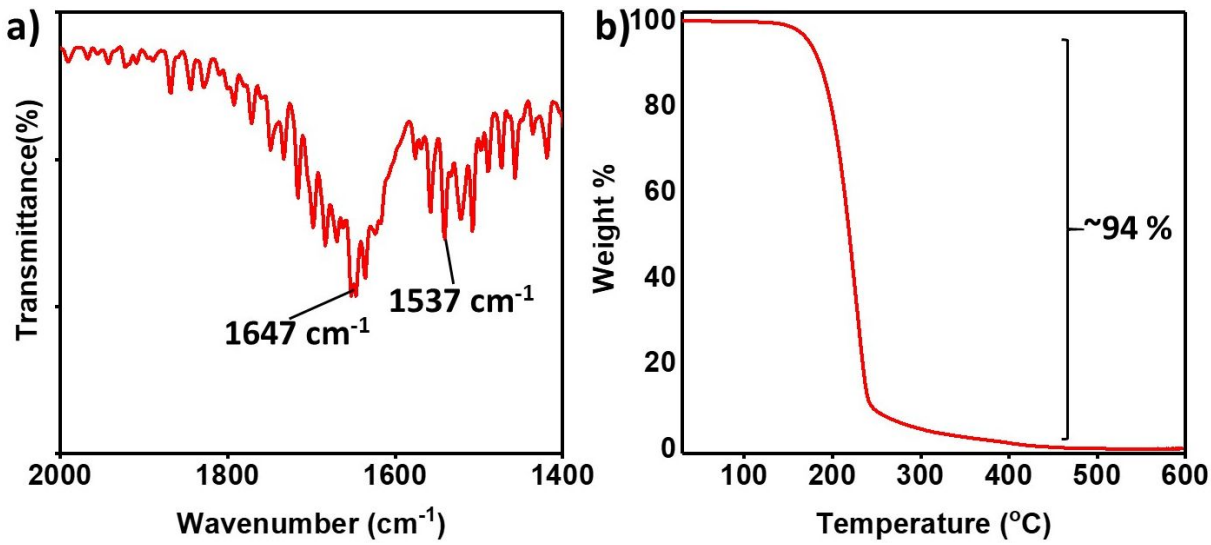

Figure S17: a) FTIR spectrum of indium palmitate (**3n**) depicting characteristic -COO$^-$ asymmetric stretching at 1647 cm^{-1} and 1537 cm^{-1}. b) TGA thermogram of indium palmitate (**3n**) displaying ~94 % loss of weight in the temperature range 152-450 °C corresponding to three palmitates.

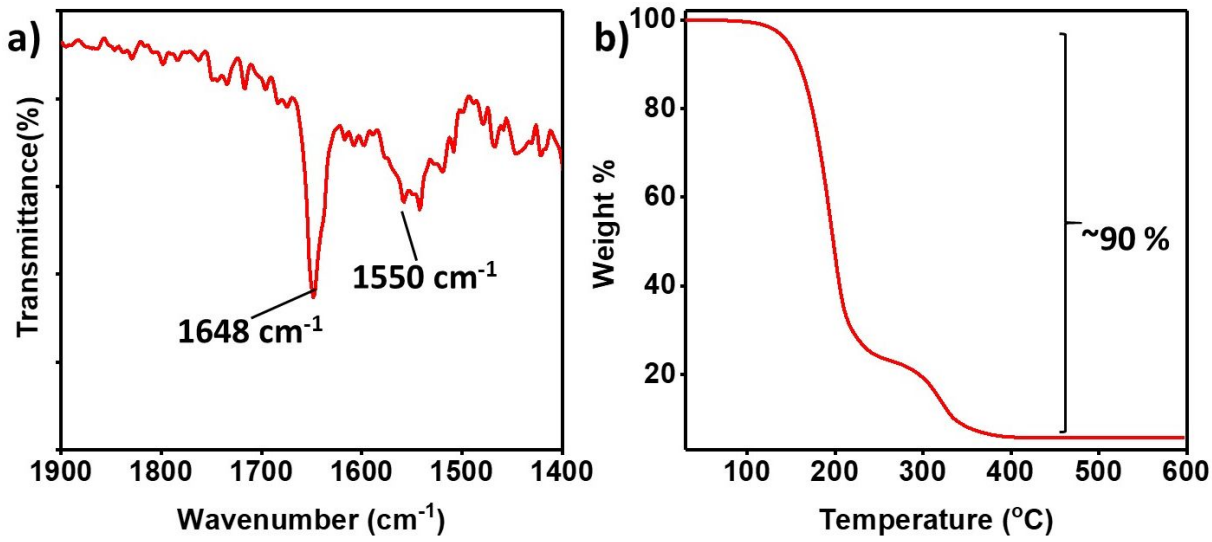

Figure S18: a) FTIR spectrum of indium laurate (**3o**) showing characteristic -COO$^-$ asymmetric stretching at 1648 cm^{-1} and 1550 cm^{-1}. b) TGA thermogram of indium laurate (**3o**) displaying ~90 % loss of weight in the temperature range 130-400 °C corresponding to three laurates.

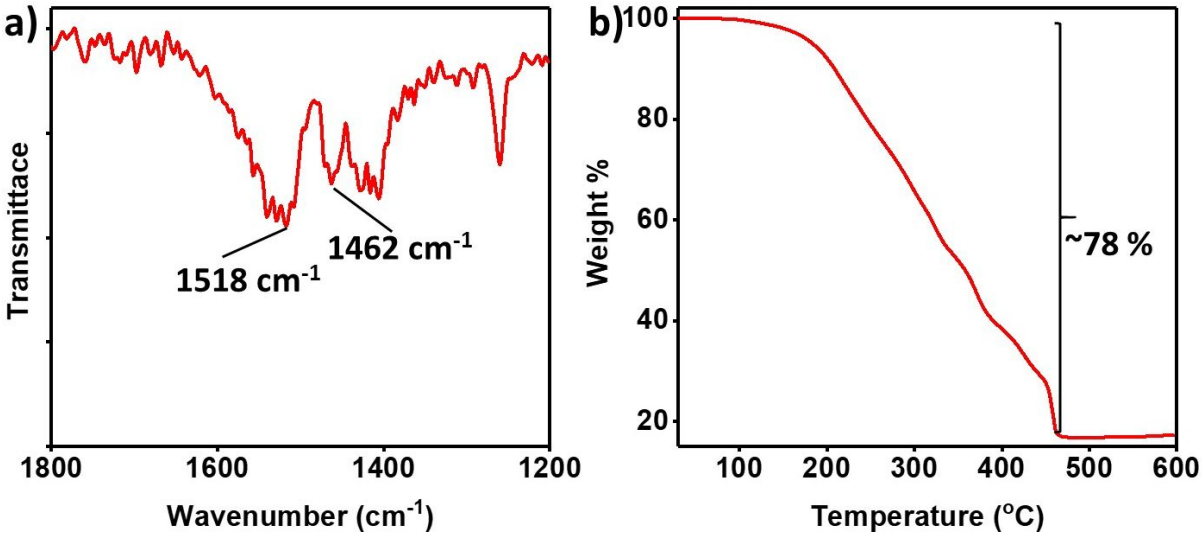

Figure S19: a) FTIR spectrum of lead oleate (**3p**) showing characteristic -COO$^-$ asymmetric stretching at 1518 cm^{-1} and symmetric stretching at 1462 cm^{-1}. b) TGA thermogram of lead oleate (**3p)** showing ~78 % loss of weight in the temperature range 170-470 ^{o}C corresponding to two oleates.

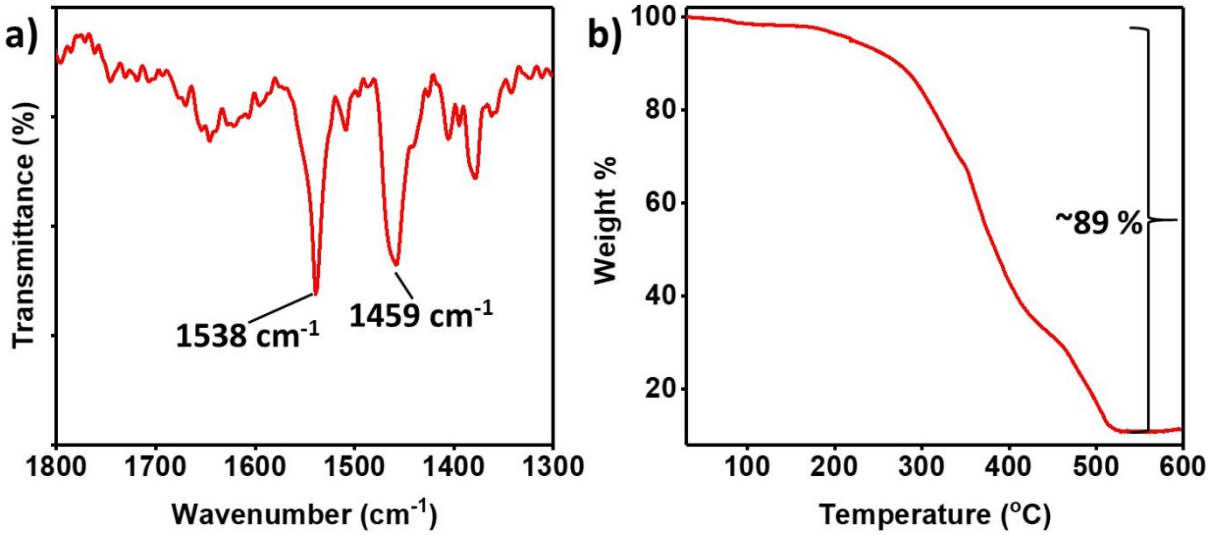

Figure S20: a) FTIR spectrum of magnesium stearate (**3q**) depicting characteristic -COO$^-$ asymmetric stretching at 1538 cm^{-1} and symmetric stretching at 1459 cm^{-1}. b) TGA thermogram of magnesium stearate (**3q)** showing ~89 % loss of weight in temperature range 177-520 ^{o}C corresponding to two stearates.

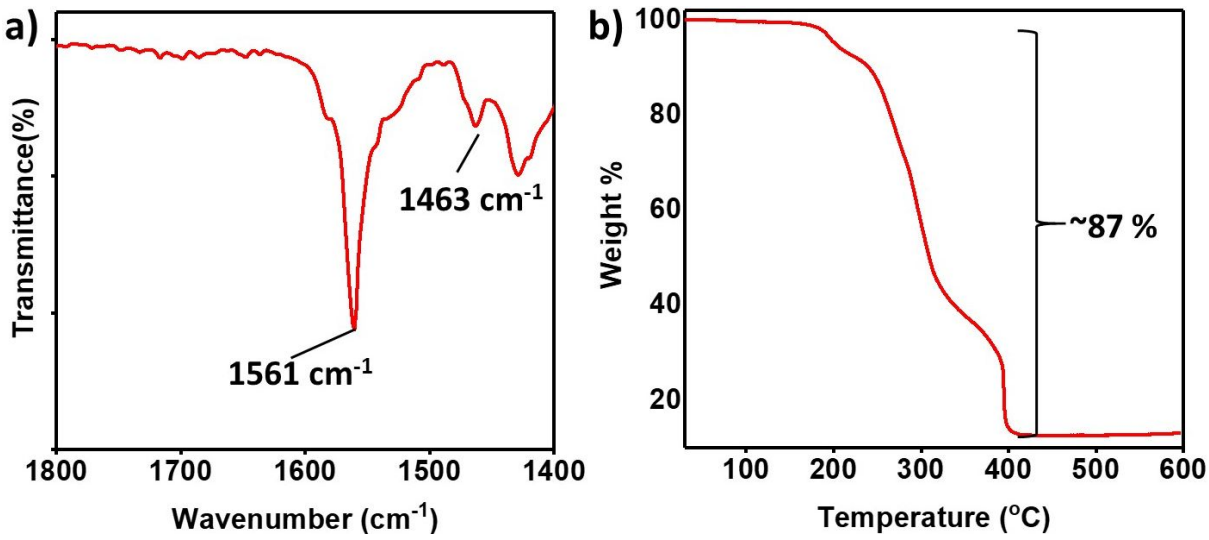

Figure S21: a) FTIR spectrum of manganese stearate (**3r**) showing characteristic m-COO^- asymmetric stretching at 1561 cm^{-1} and symmetric stretching at 1463 cm^{-1}. b) TGA thermogram of manganese stearate (**3r)** showing ~87 % loss of weight in temperature range 130-450 °C corresponding to two stearates.

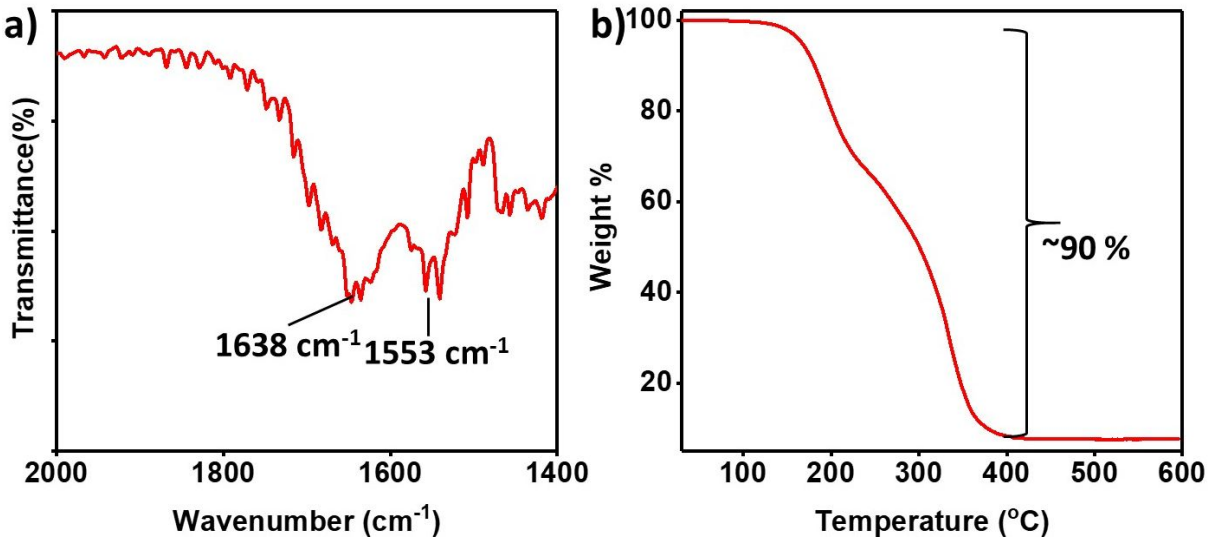

Figure S22: a) FTIR spectrum of nickel stearate (**3s**) depicting characteristic -COO^- asymmetric stretching at 1638 cm^{-1} and 1553 cm^{-1}. b) TGA thermogram of nickel stearate (**3s)** displaying ~90 % loss of weight in temperature range 150-410 °C corresponding to two stearates.

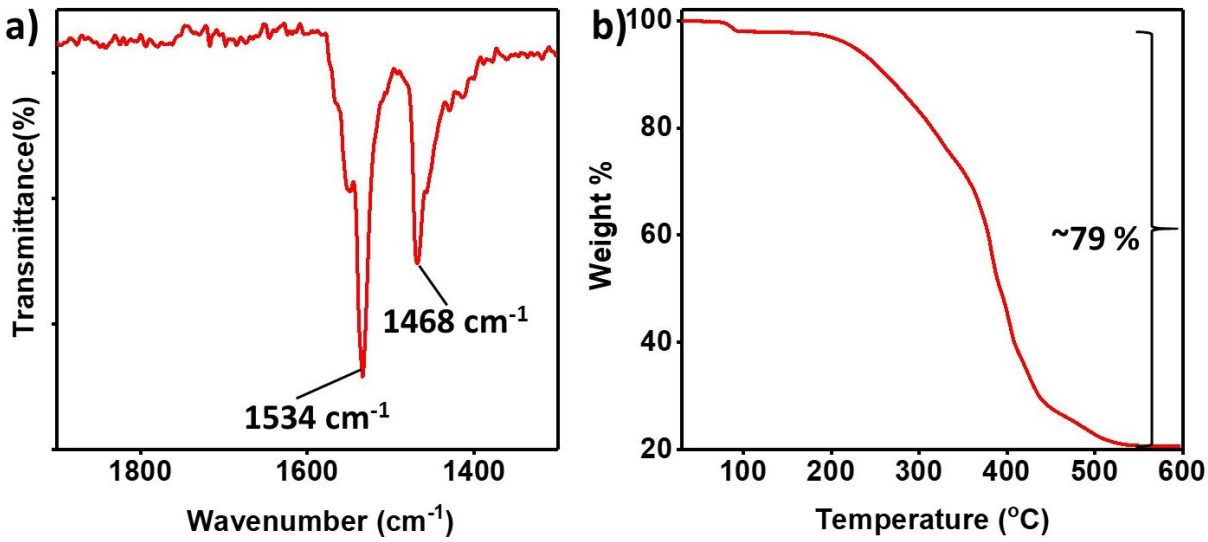

Figure S23: a) FTIR spectrum of gadolinium stearate (**3t**) showing characteristic -COO$^-$ asymmetric stretching at 1534 cm^{-1} and symmetric stretching at 1468 cm^{-1}. b) TGA thermogram of gadolinium stearate (**3t)** showing ~79 % loss of weight in the temperature range 200-540 ^{o}C corresponding to three stearates.

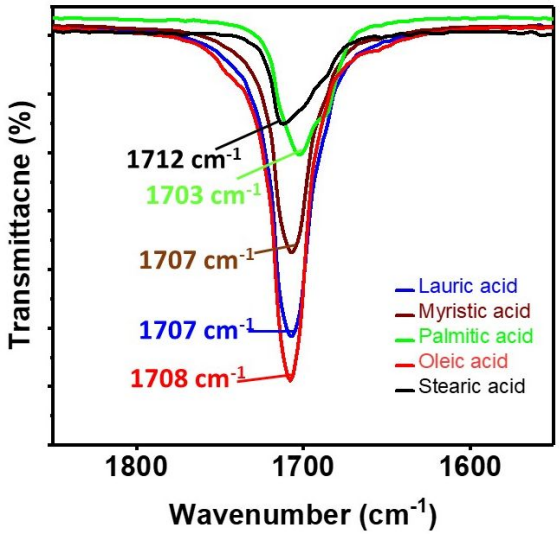

Figure. S24: FTIR spectrum of pristine stearic acid (black), oleic acid (red), palmitic acid s(green), myristic acid (wine red) and lauric acid (blue) showing the characteristic asymmetric C=O stretching at 1703-1712 cm^{-1}.

5. ^{1}H and ^{13}C NMR spectra:

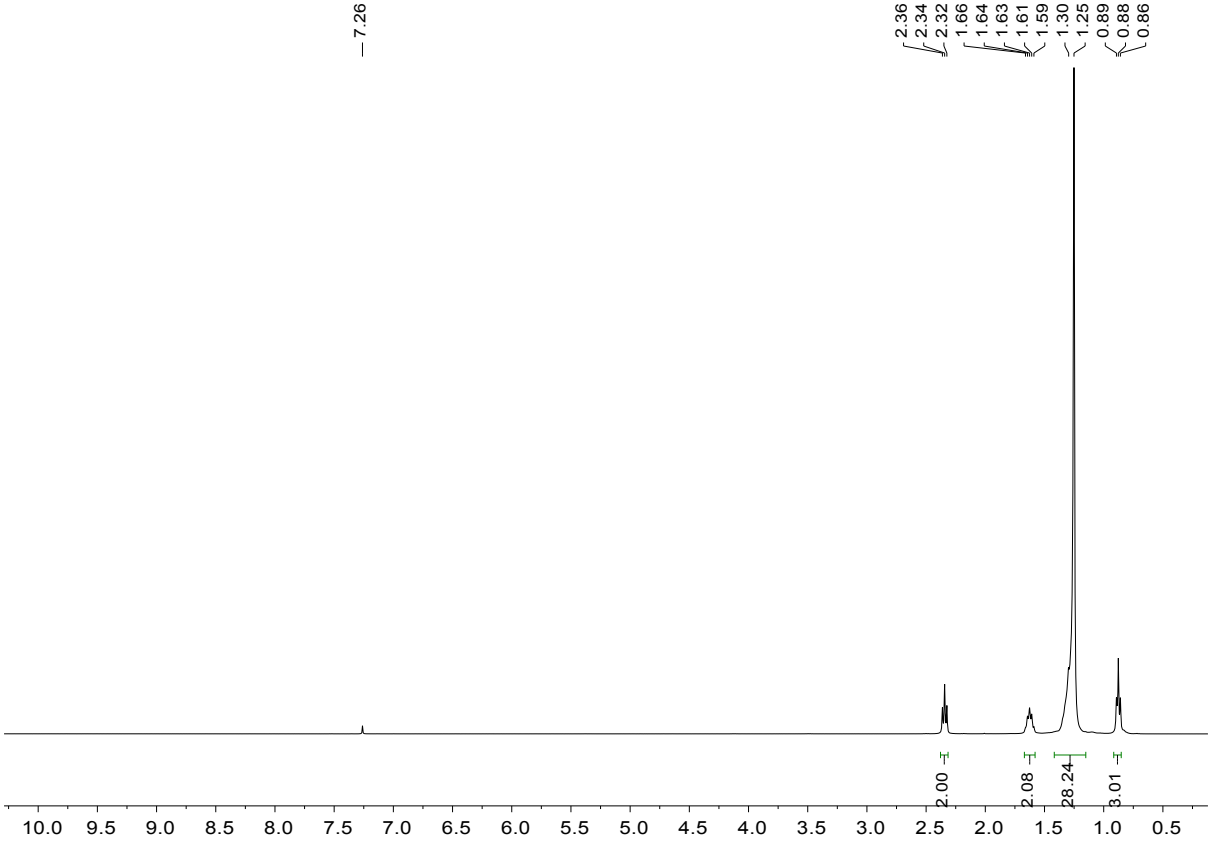

Figure S25**:** ^{1}H NMR of gallium stearate **(3b)** ($CDCl_3$, 400 MHz)

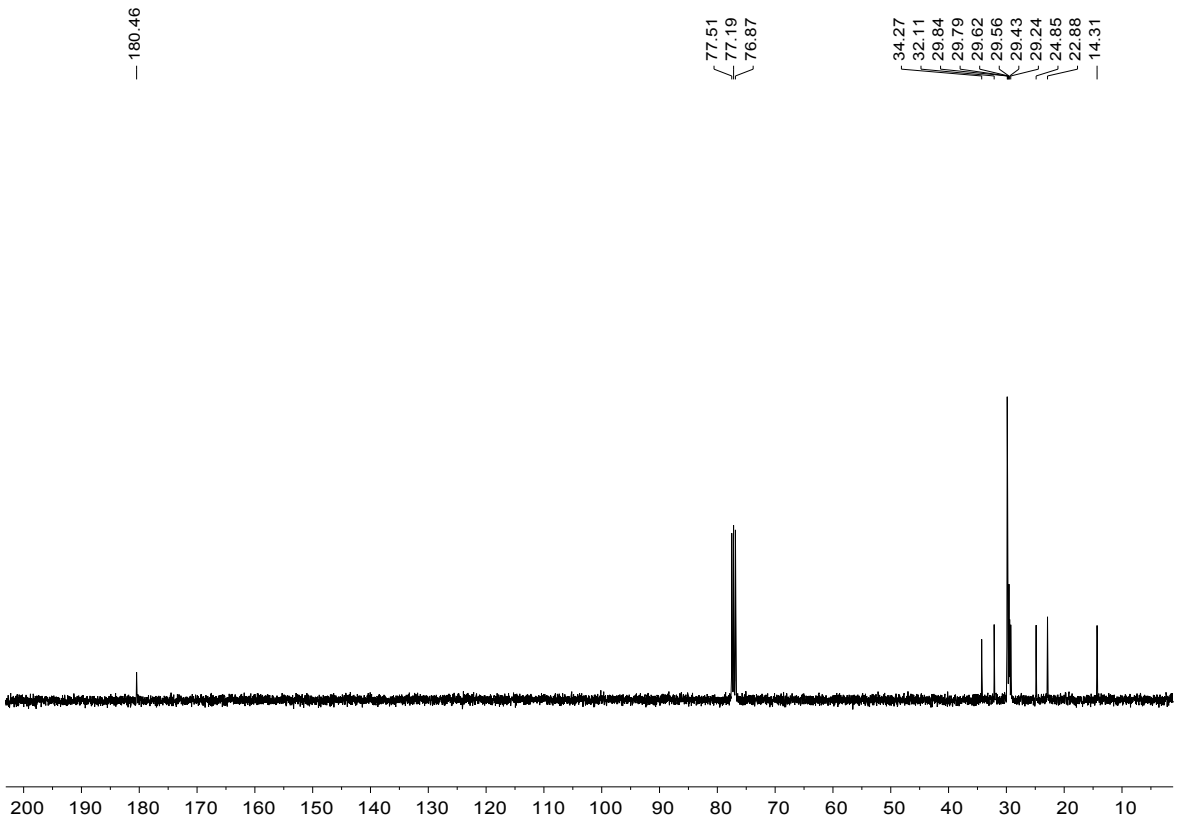

Figure S26**:** ^{13}C NMR of gallium stearate **(3b)** ($CDCl_3$,100 MHz)

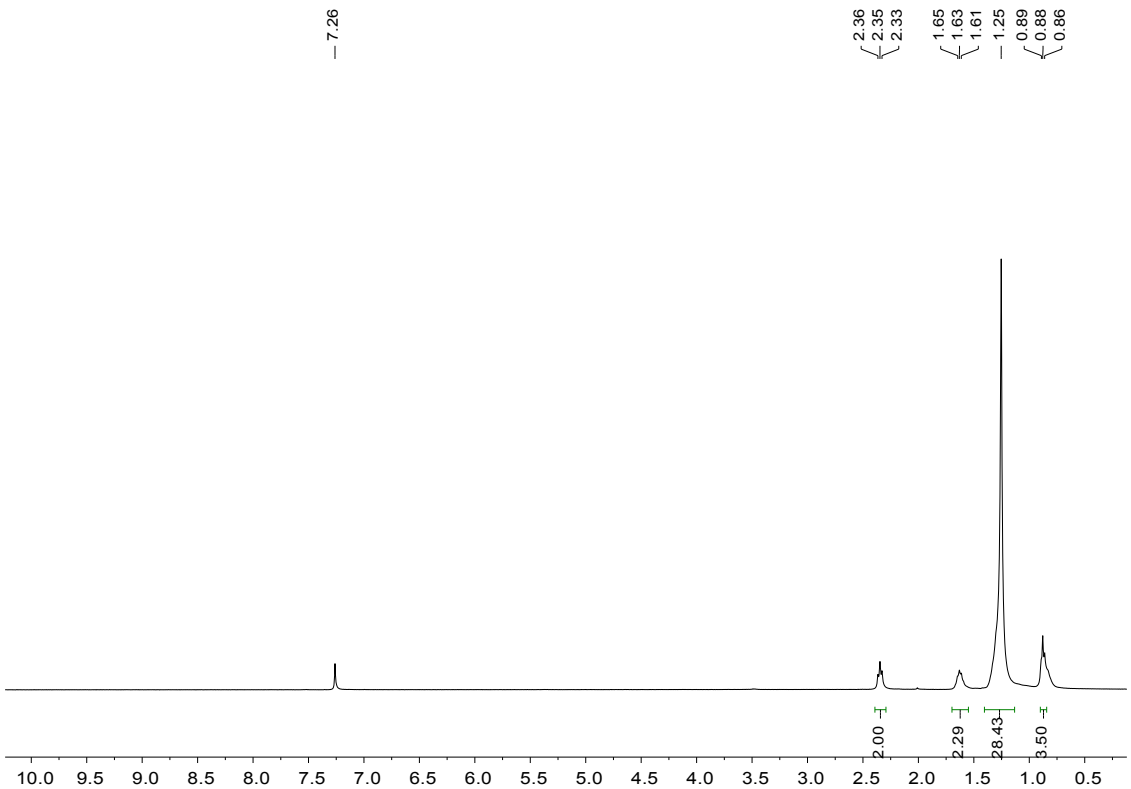

Figure S27: ^{1}H NMR of lead stearate **(3c)** ($CDCl_3$, 400 MHz)

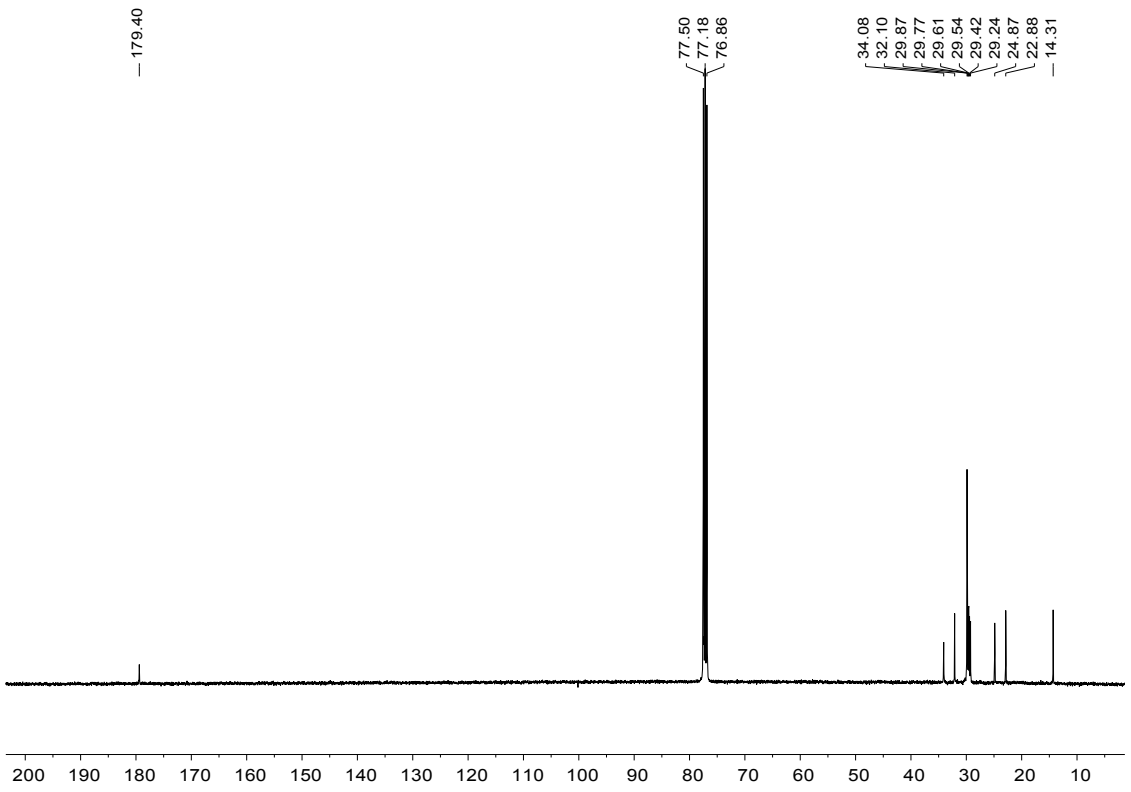

Figure S28: ^{13}C NMR of lead stearate **(3c)** ($CDCl_3$, 100 MHz)

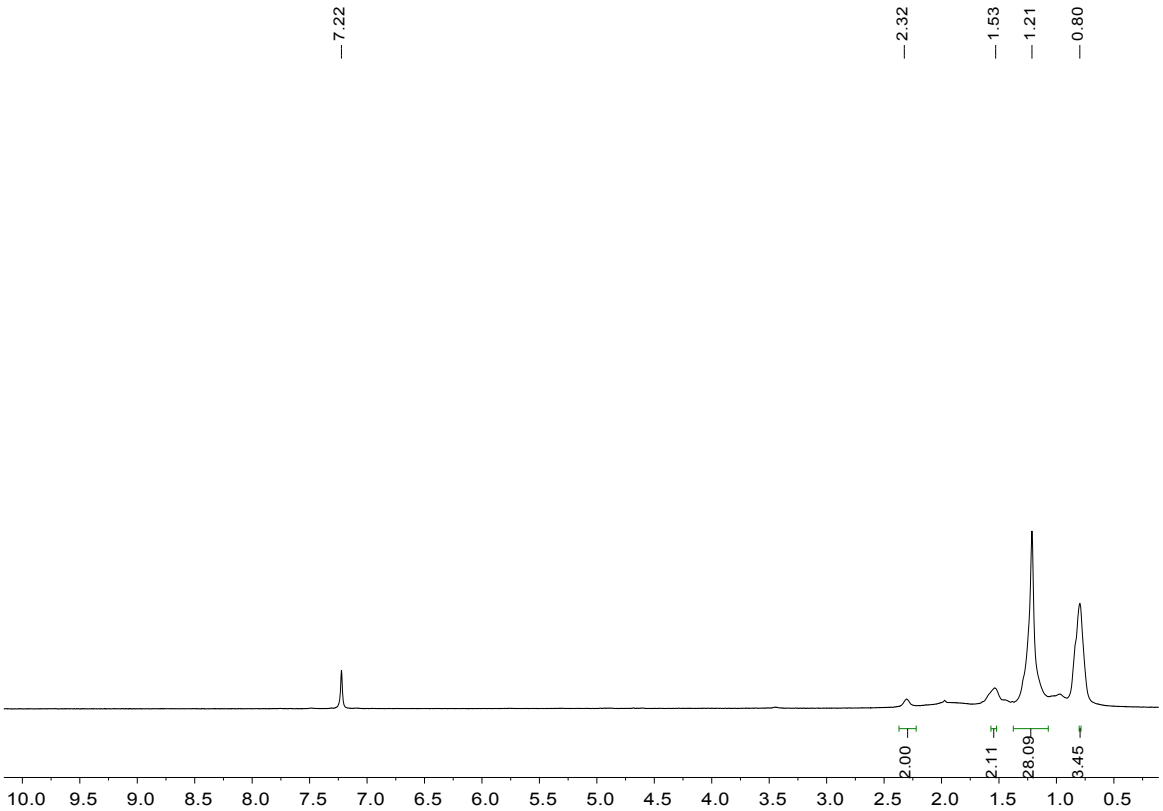

Figure S29: ^{1}H NMR of silver stearate **(3d)** ($CDCl_3$, 400 MHz)

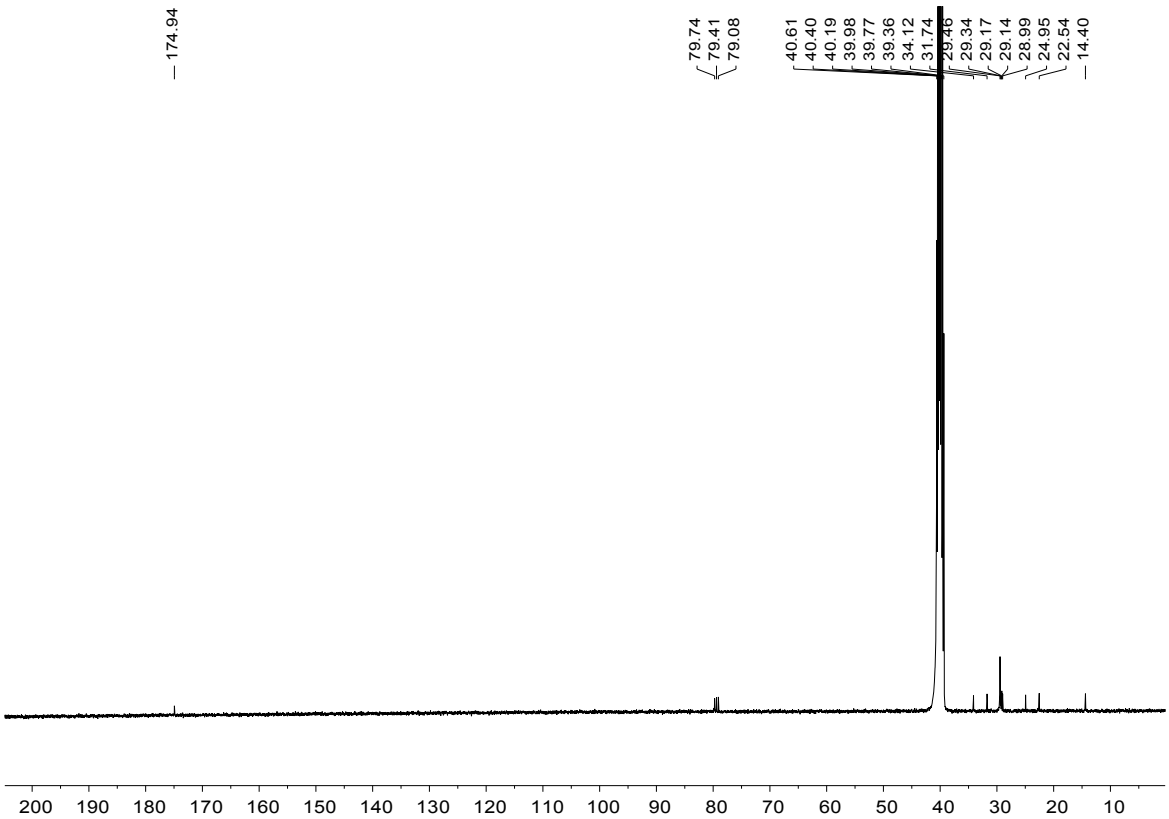

Figure S30: ^{13}C NMR of silver stearate **(3d)** ($CDCl_3$, DMSO-d6, 100 MHz)

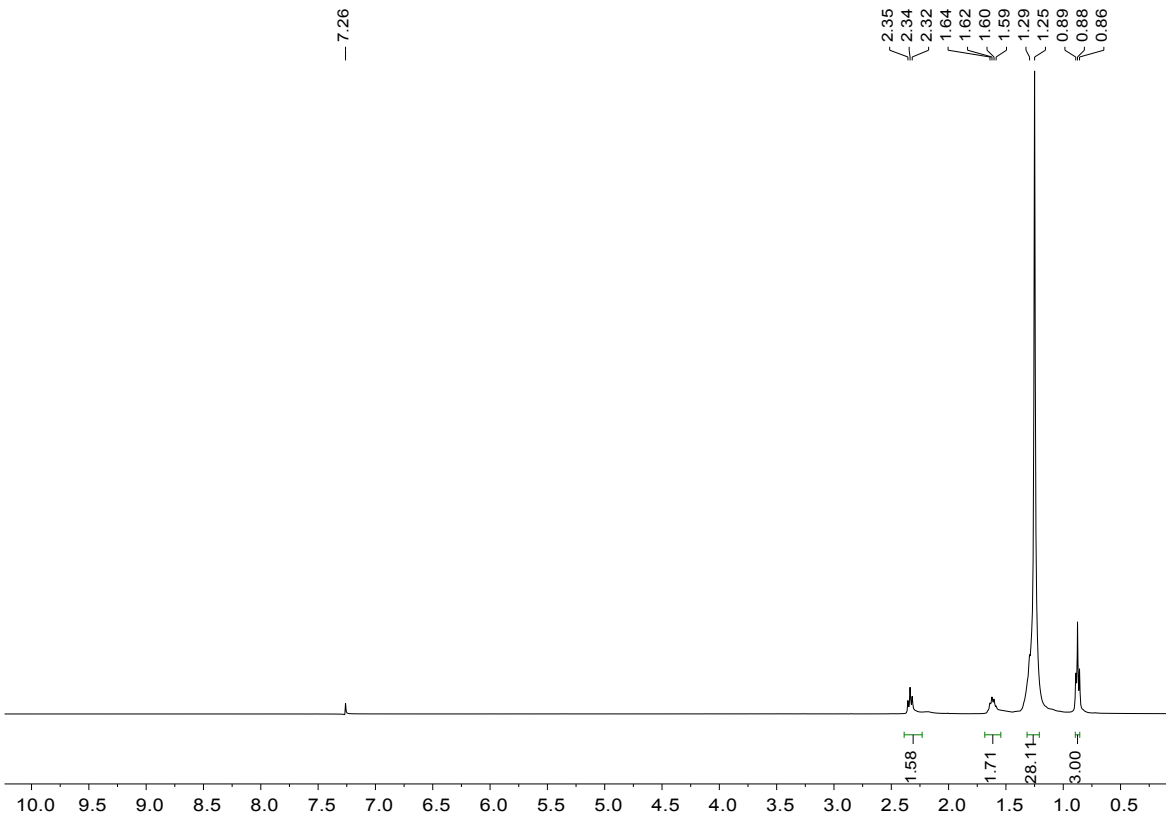

Figure S31: ^{1}H NMR of aluminum stearate **(3e)** ($CDCl_3$, 400 MHz)

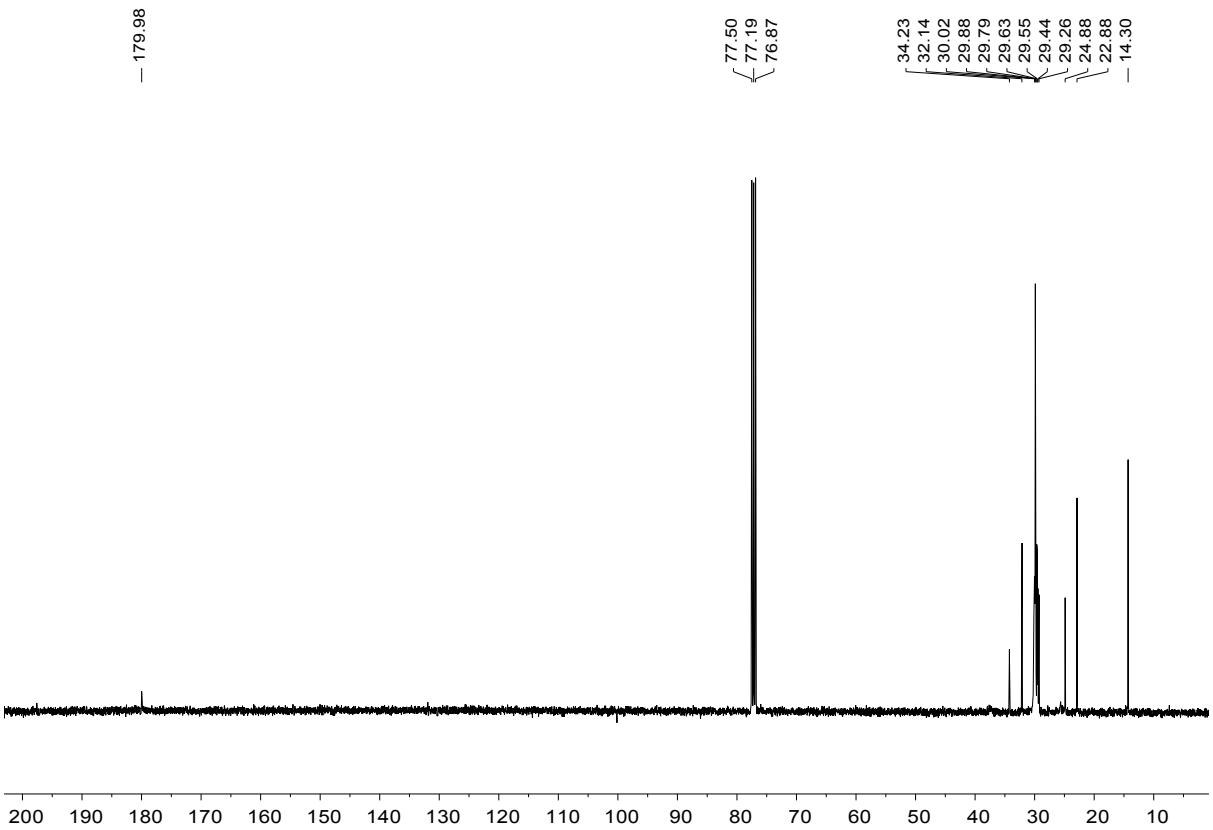

Figure S32: ^{13}C NMR of aluminum stearate **(3e)** ($CDCl_3$, 100 MHz)

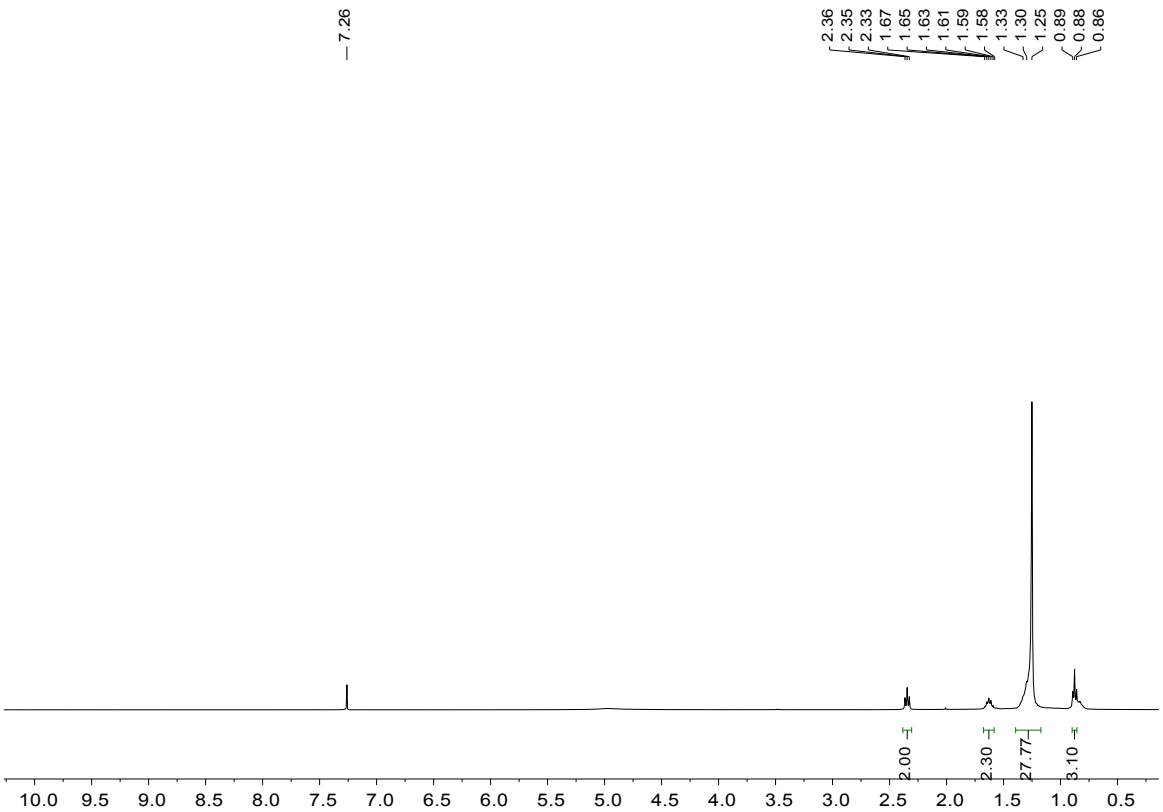

Figure S33: ^{1}H NMR of zinc stearate **(3i)** ($CDCl_3$, 400 MHz)

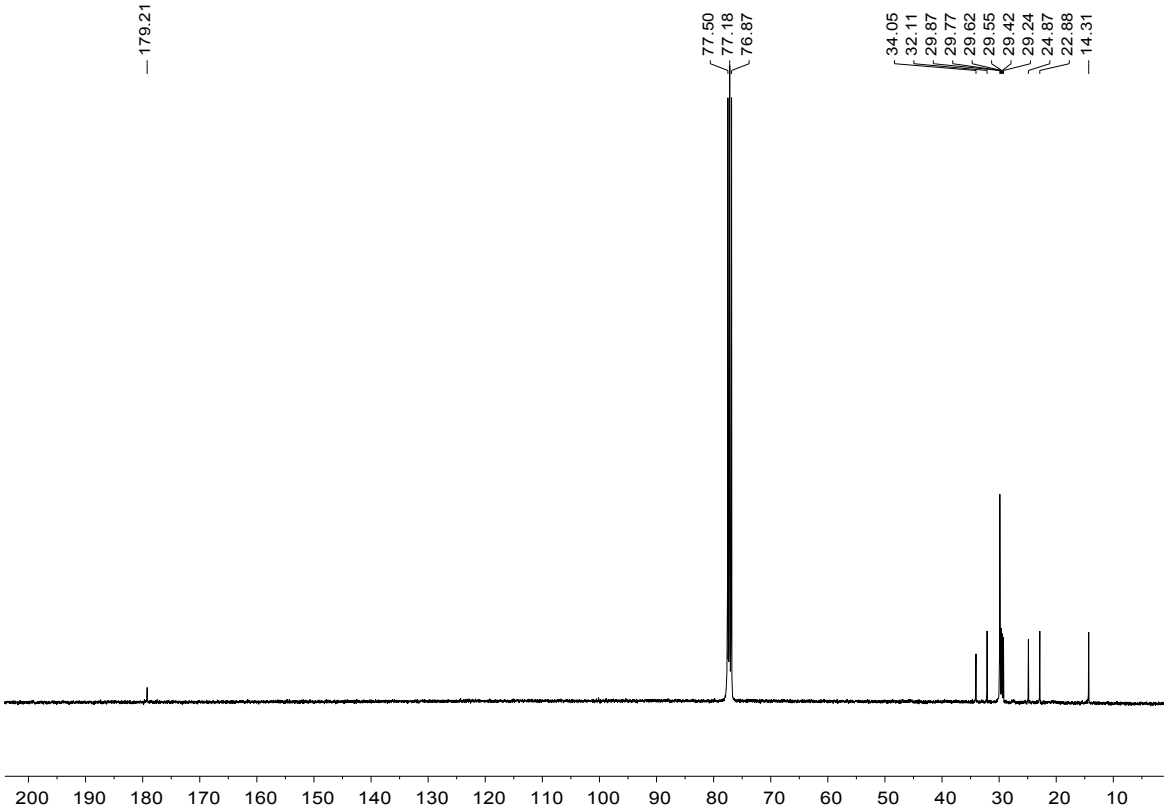

Figure S34: ^{13}C NMR of zinc stearate **(3i)** ($CDCl_3$, 100 MHz)

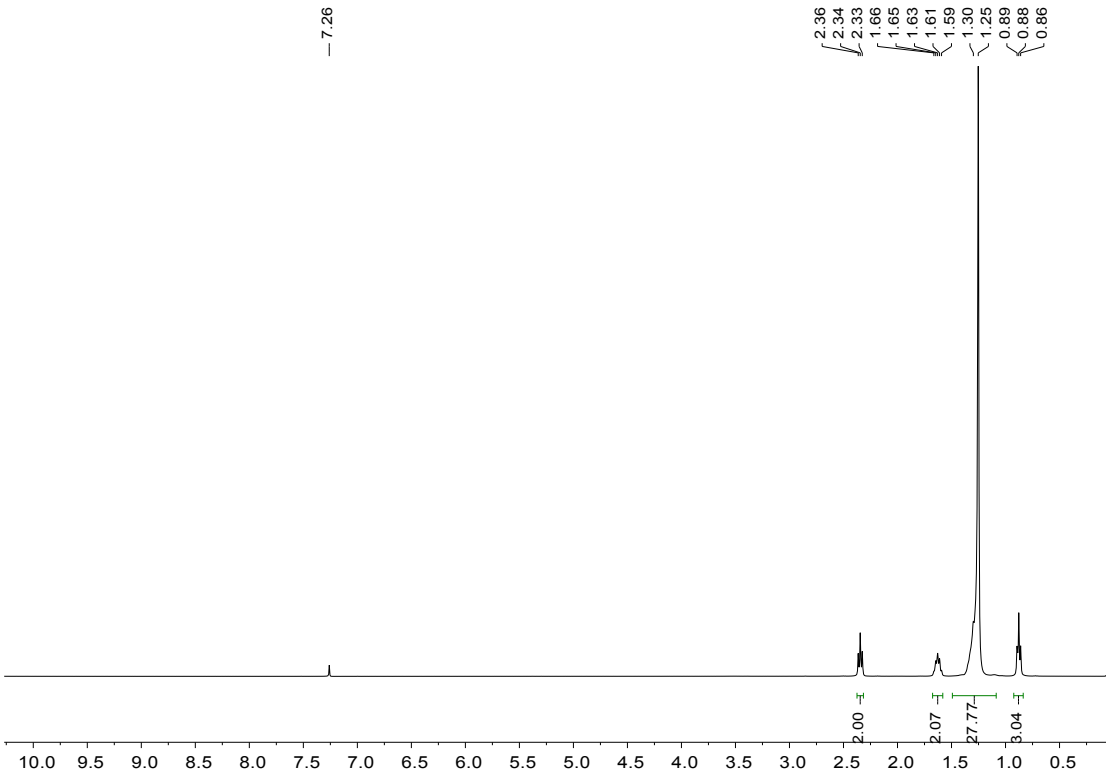

Figure S35: ^{1}H NMR of tin (II) stearate **(3j)** ($CDCl_3$, 400 MHz)

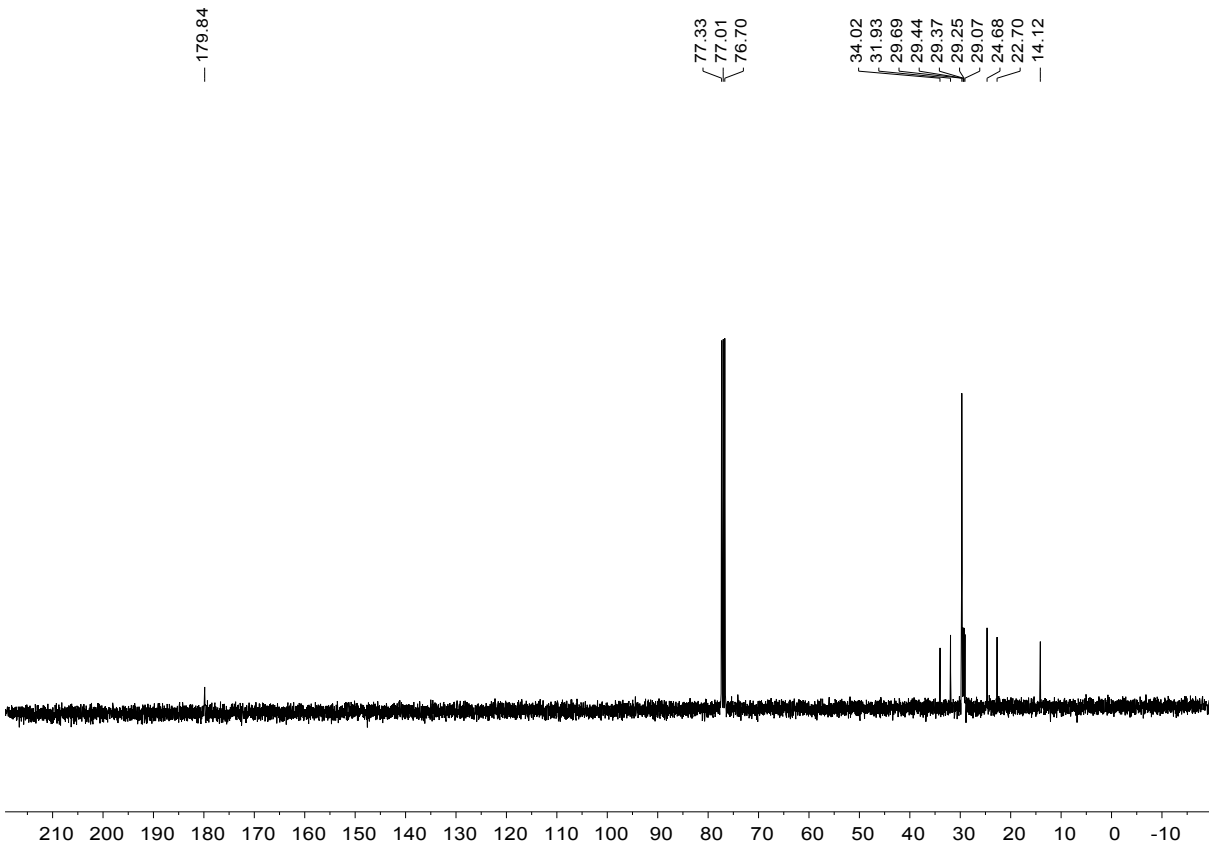

Figure S36: ^{13}C NMR of tin (II) stearate **(3j)** ($CDCl_3$, 100 MHz)

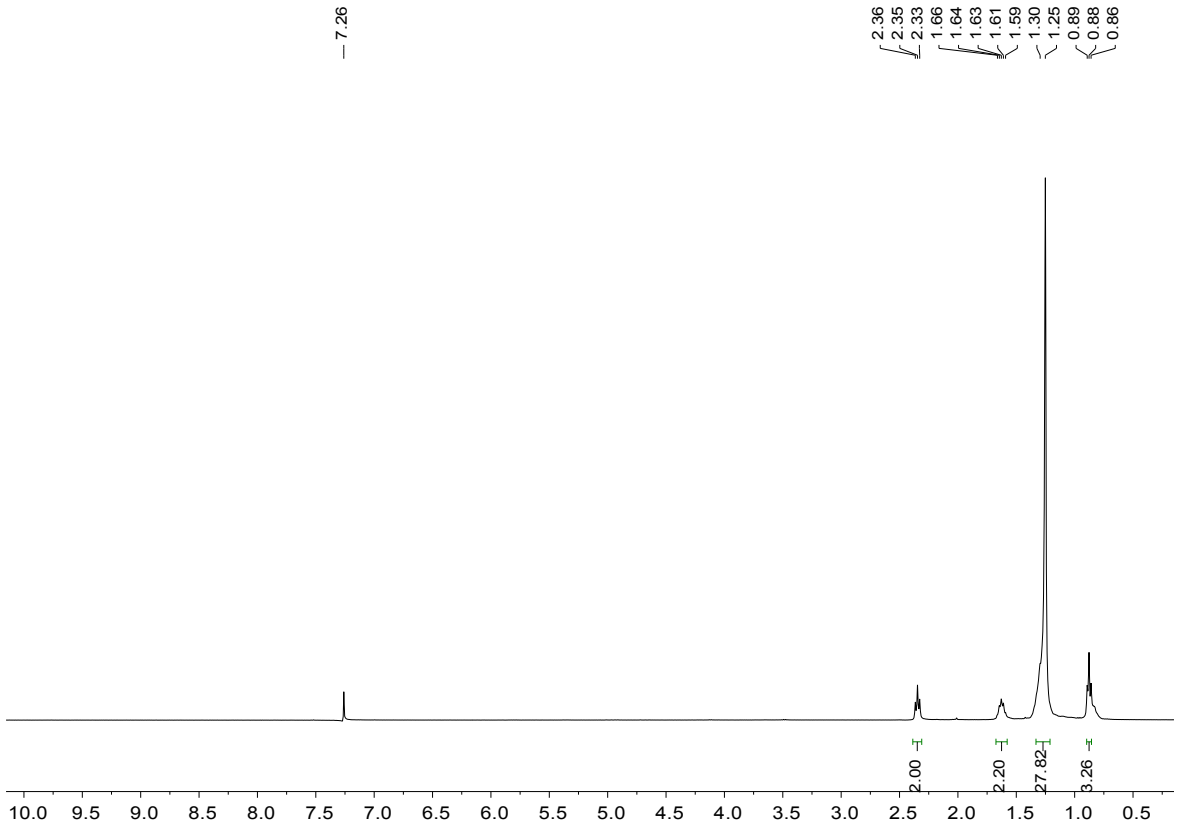

Figure S37: ^{1}H NMR of cadmium stearate **(3k)** ($CDCl_3$, 400 MHz)

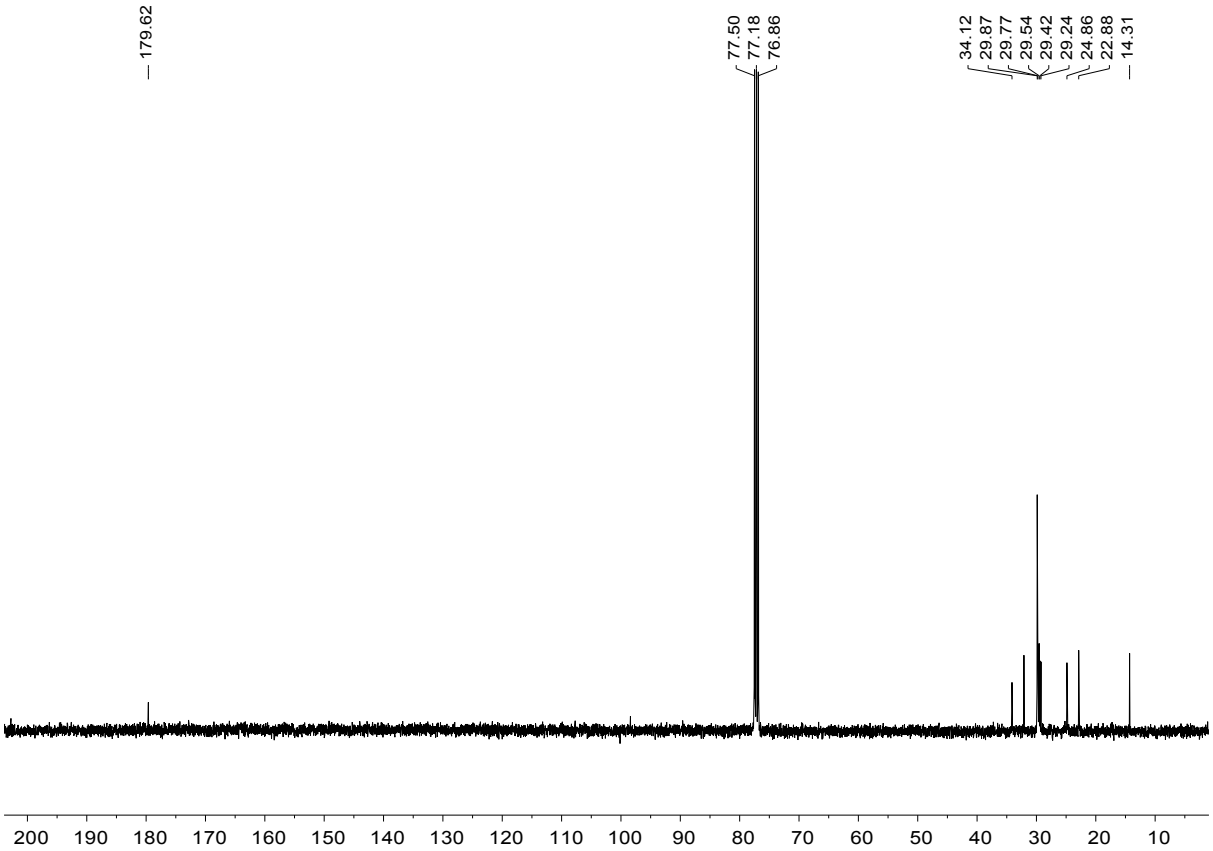

Figure S38: ^{13}C NMR of cadmium stearate **(3k)** ($CDCl_3$, 100 MHz)

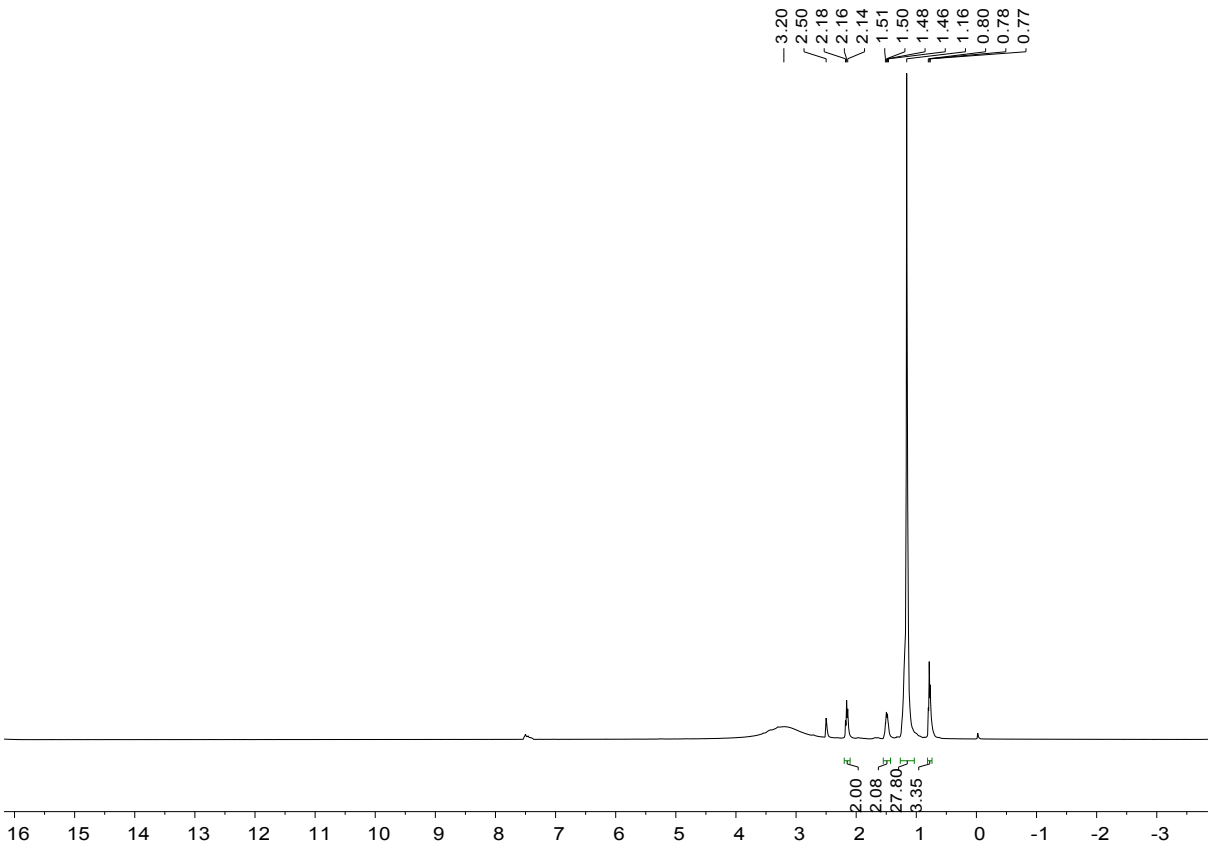

Figure S39: ^{1}H NMR of potassium stearate **(3l)** ($CDCl_3$, DMSO-d6, 400 MHz)

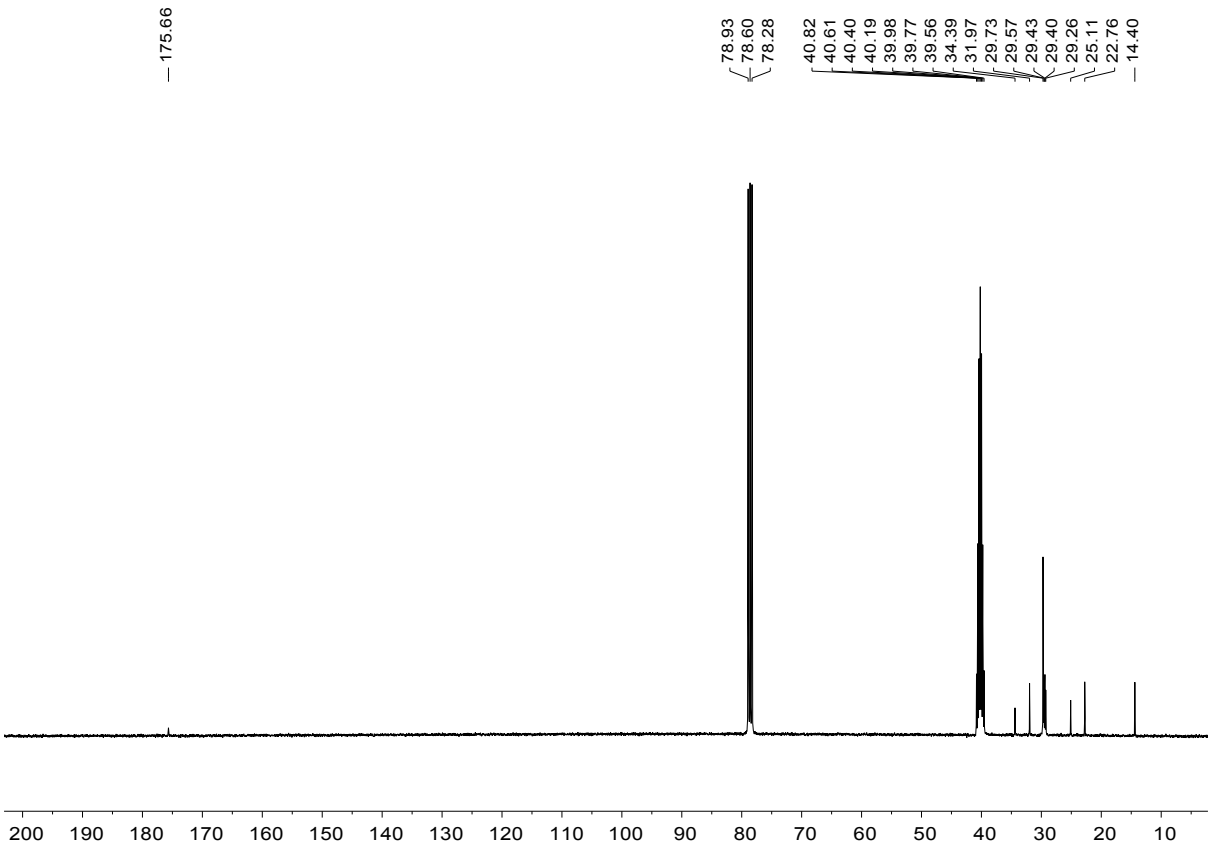

Figure S40: ^{13}C NMR of potassium stearate **(3l)** ($CDCl_3$, DMSO-d6, 100 MHz)

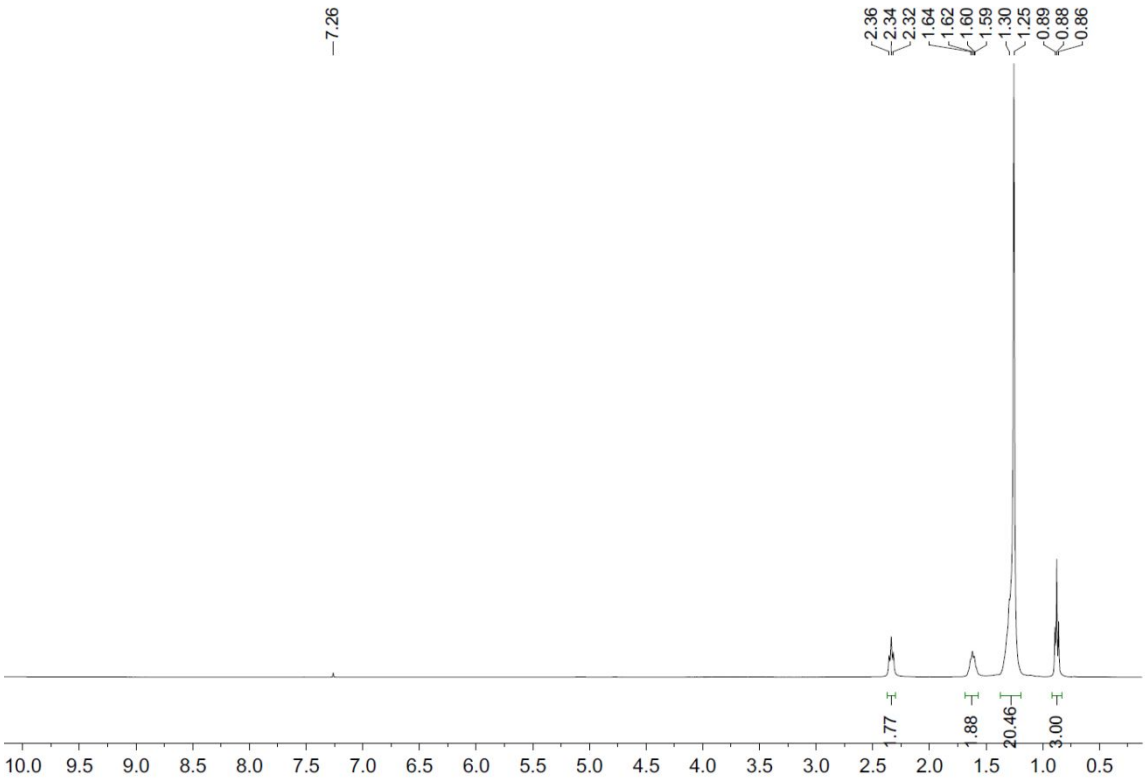

Figure S41: ^{1}H NMR of indium myristate **(3m)** ($CDCl_3$, 400 MHz)

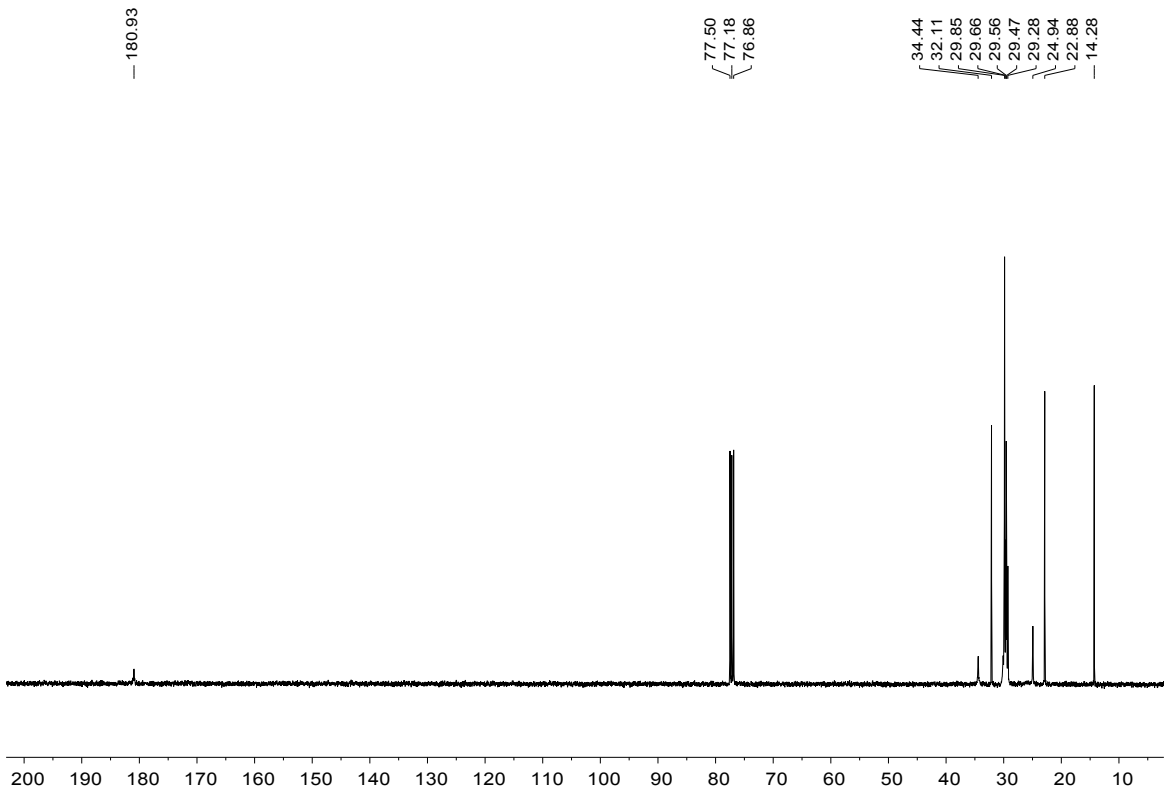

Figure S42: ^{13}C NMR of indium myristate **(3m)** ($CDCl_3$, 100 MHz)

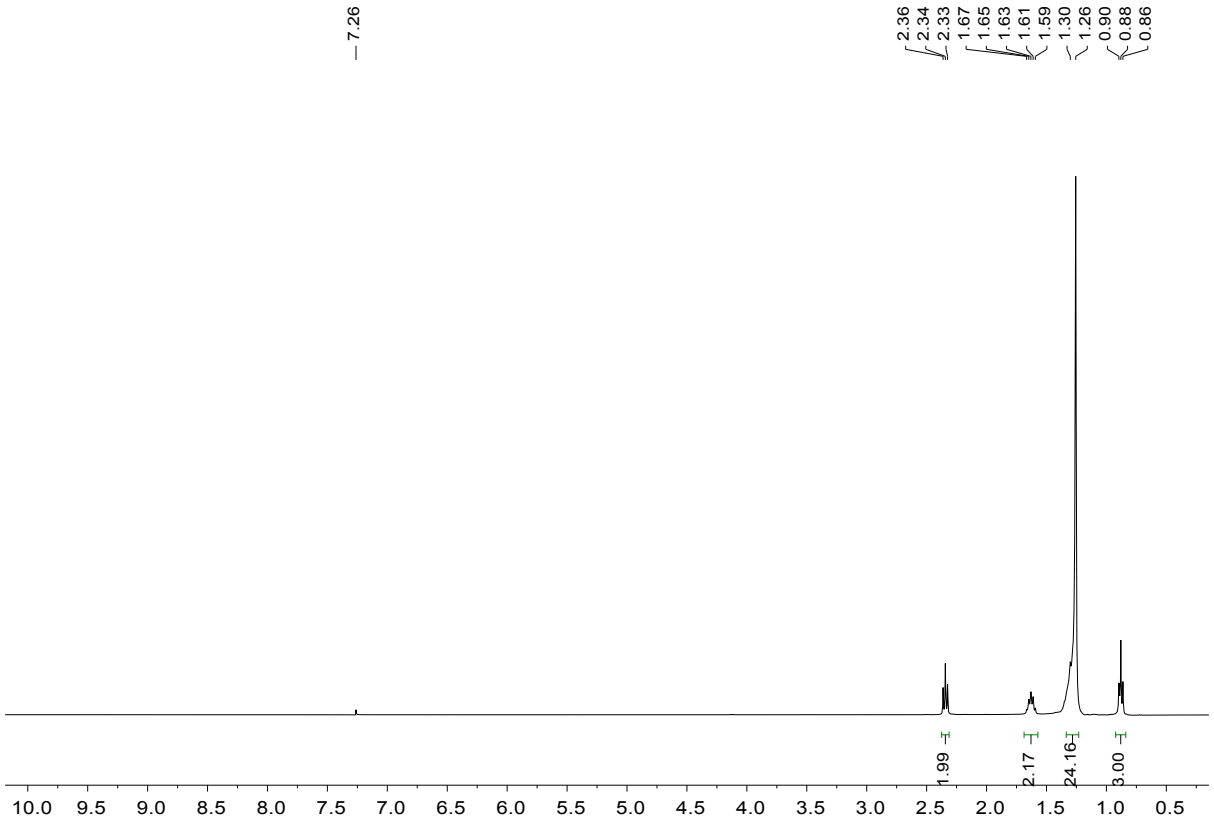

Figure S43**:** ^{1}H NMR of indium palmitate **(3n)** ($CDCl_3$, 400 MHz)

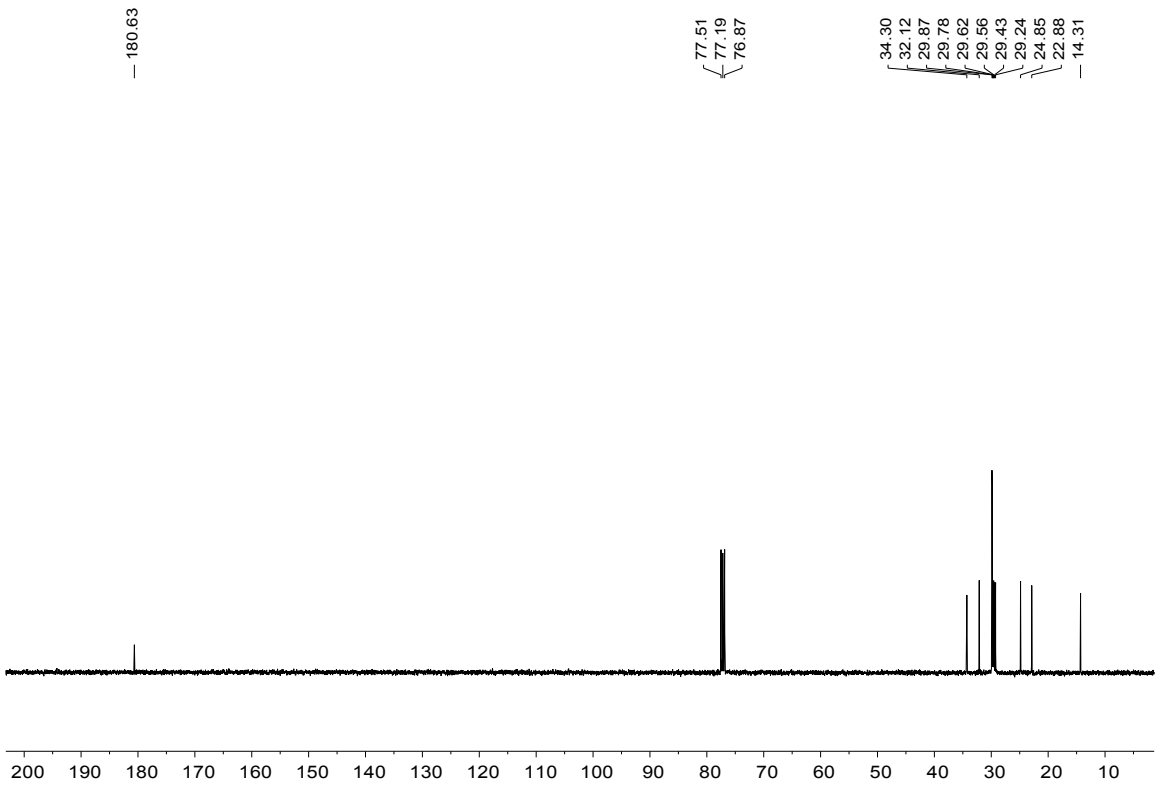

Figure S44: ^{13}C NMR of indium palmitate **(3n)** ($CDCl_3$, 100 MHz)

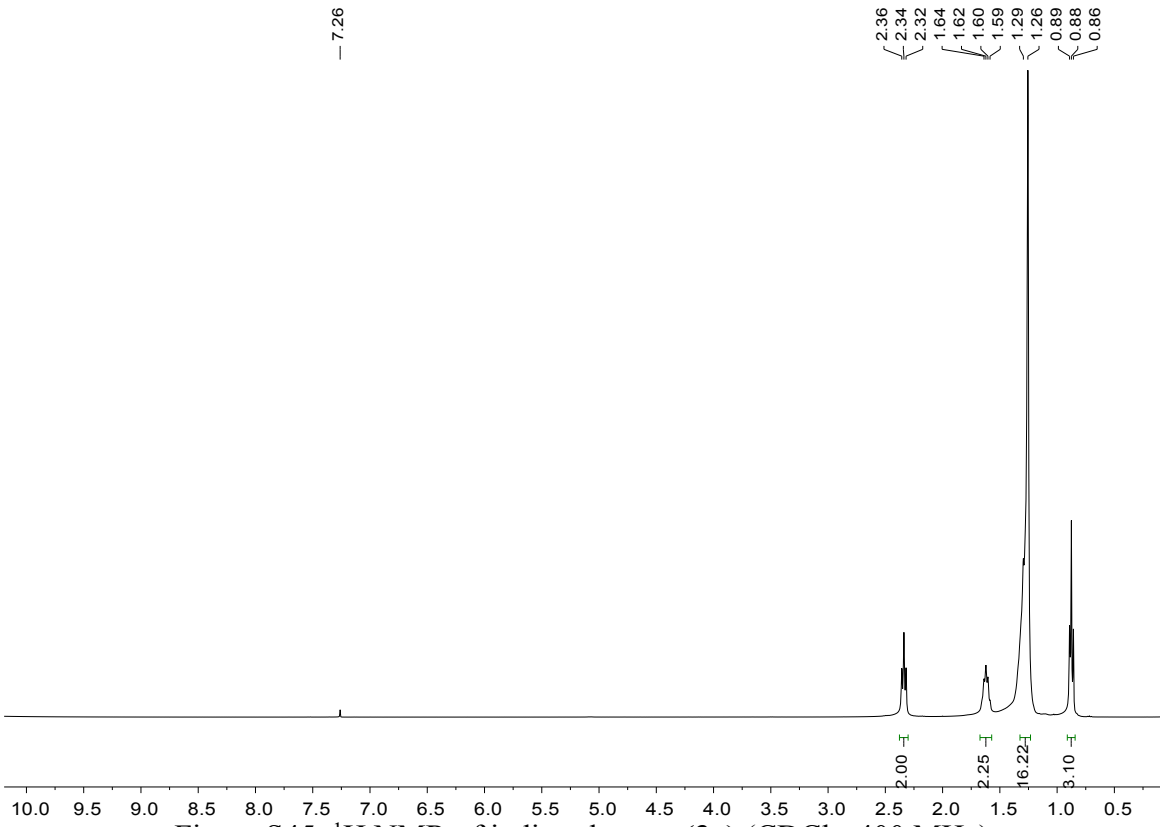

Figure S45: ^{1}H NMR of indium laurate **(3o)** ($CDCl_3$, 400 MHz)

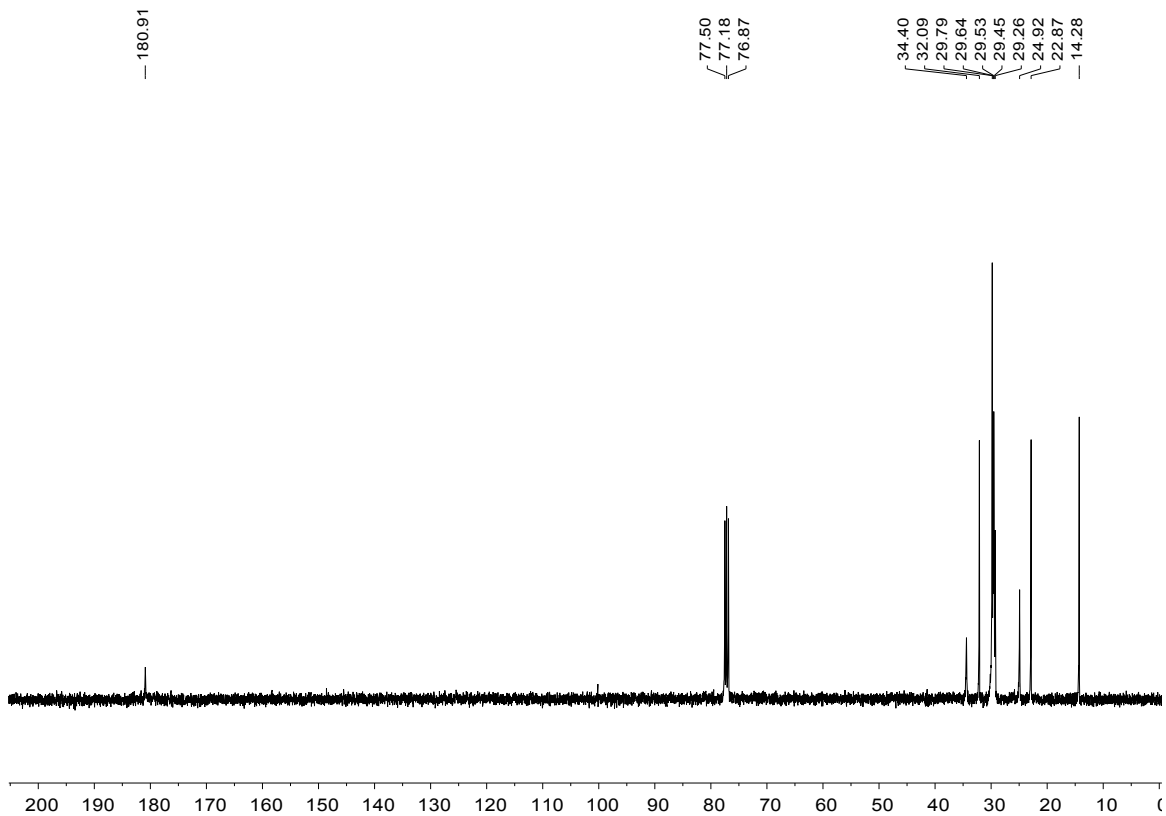

Figure S46: ^{13}C NMR of indium laurate **(3o)** ($CDCl_3$, 100 MHz)

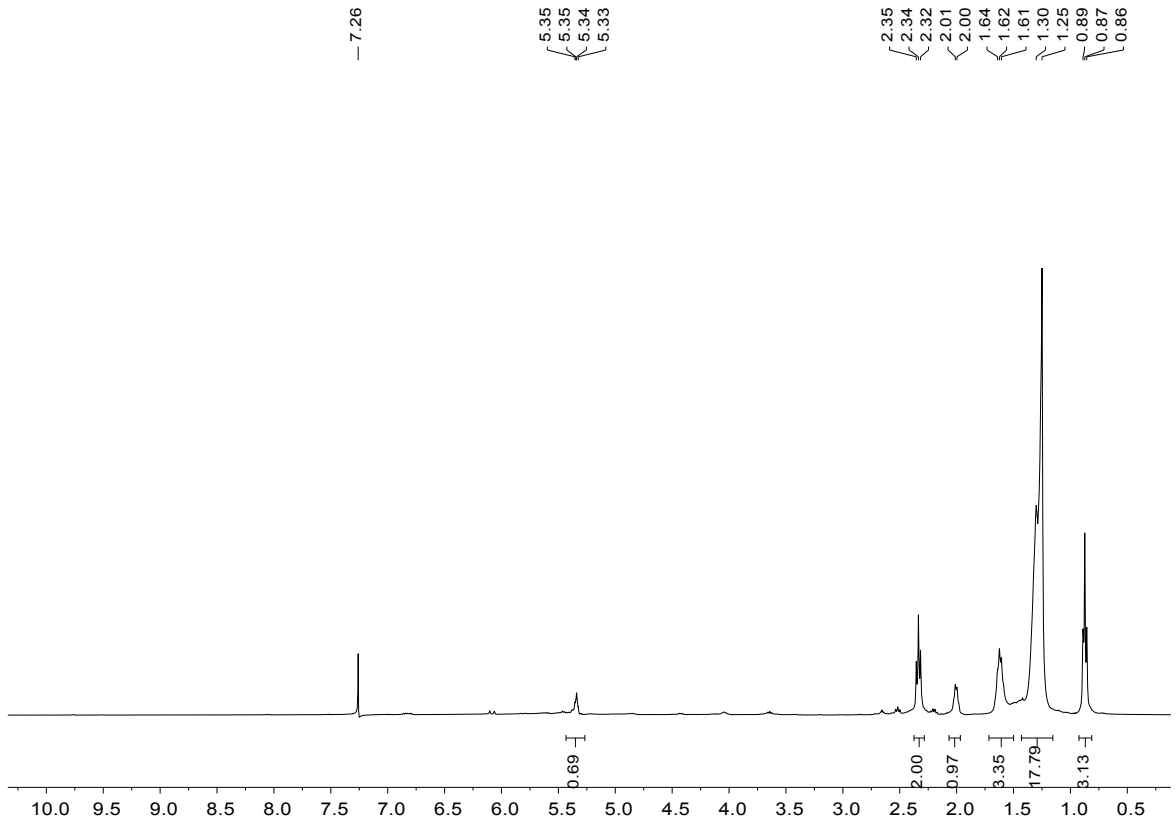

Figure S47: ^{1}H NMR of lead oleate **(3p)** ($CDCl_3$, 400 MHz)

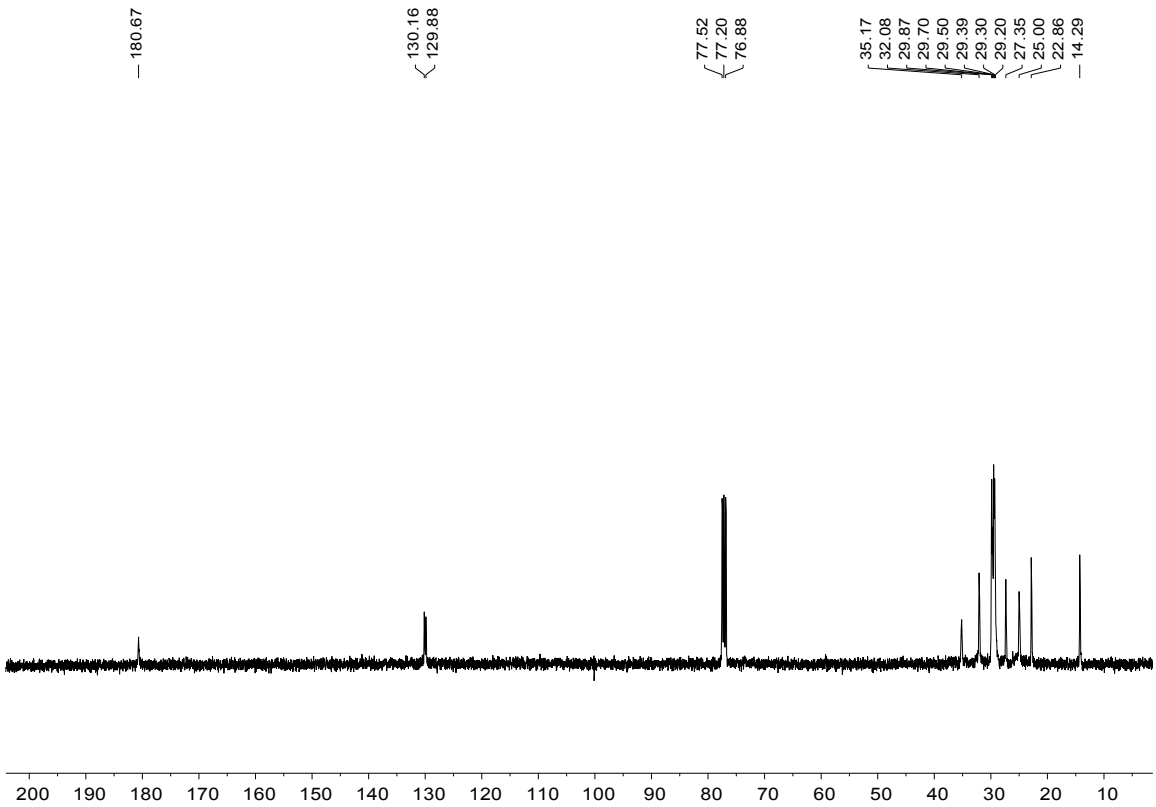

Figure S48: ^{13}C NMR of lead oleate **(3p)** ($CDCl_3$, 100 MHz)

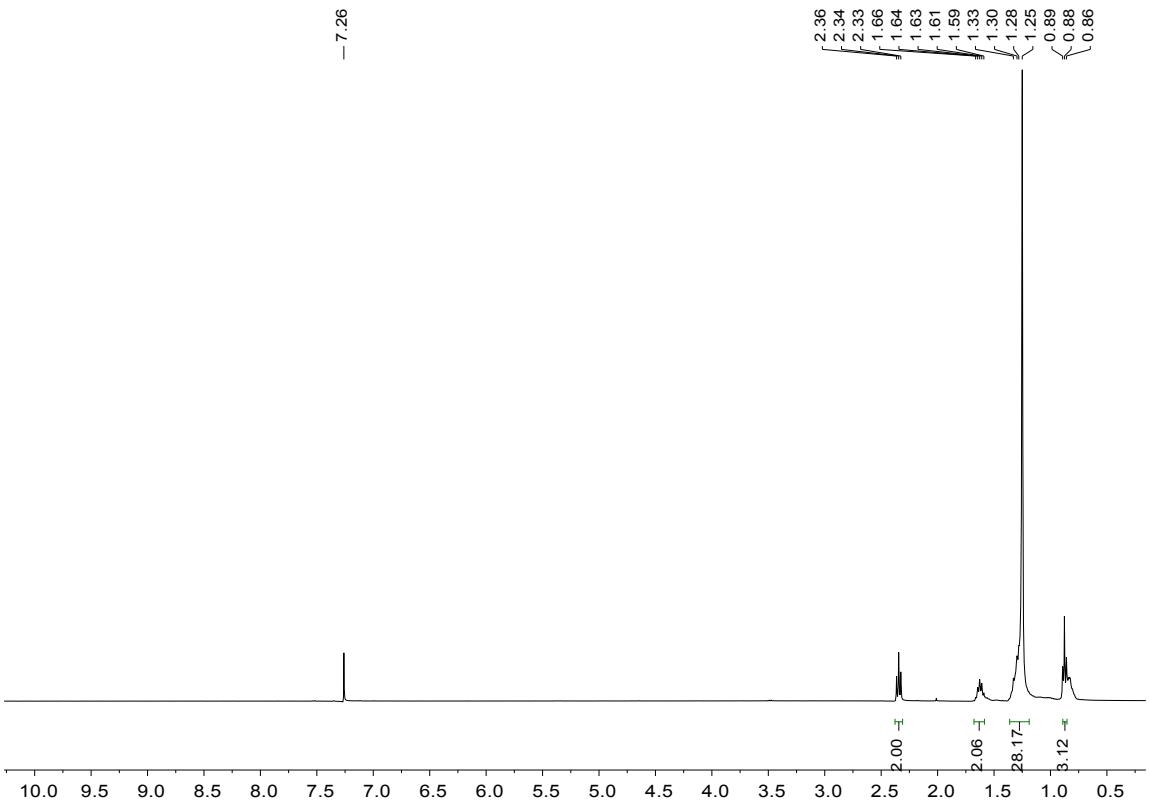

Figure S49: ^{1}H NMR of magnesium stearate **(3q)** ($CDCl_3$, 400 MHz)

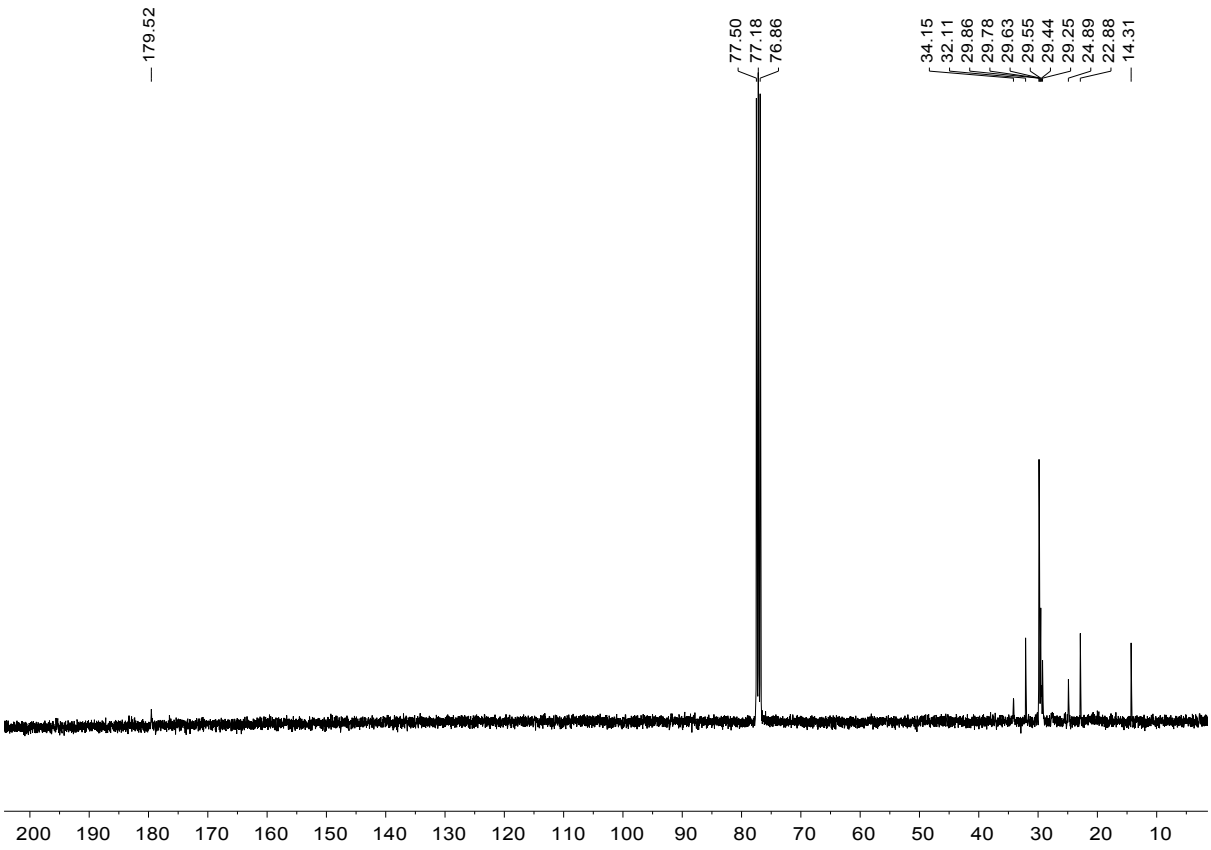

Figure S50: ^{13}C NMR of magnesium stearate **(3q)** ($CDCl_3$, 100 MHz)

6. Photographs of colloidal dispersion of semiconductor nanocrystals in hexane.

Figure S51: Colloidal dispersion of $CsPbBr_3$ NCs, $CuFeS_2$ NCs, PbS NCs, Ag_2S NCs and InP NCs (respectively from left to right) in hexane.

7. Characterization of $CsPbBr_3$ NCs as a representative example.

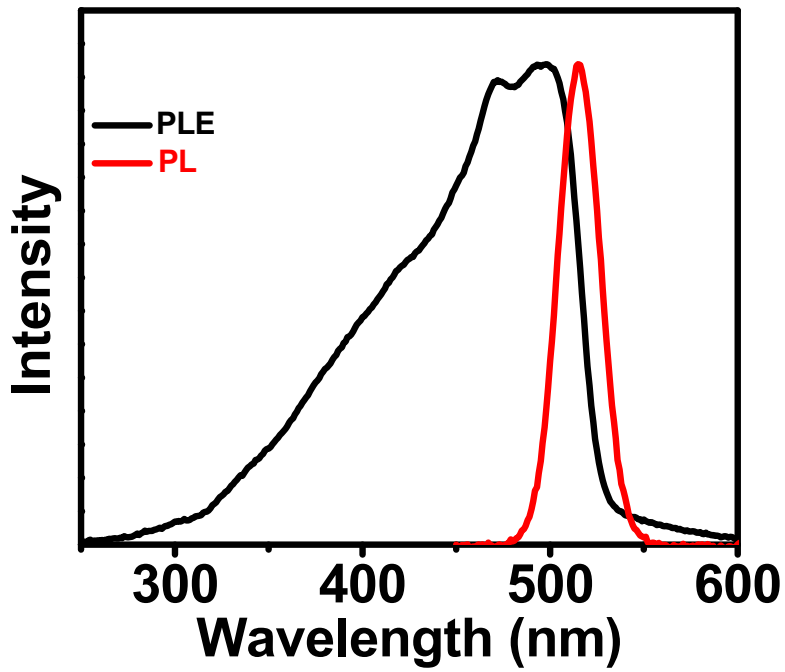

Figure S52: Photoluminescence excitation (PLE, black line) spectrum of $CsPbBr_3$ NCs in hexane with maximum (λ_{ex}) at 472 nm (emission: 515 nm). The corresponding photoluminescence (PL, red line) emission spectrum exhibiting emission maximum (λ_{em}) at 515 nm (excitation: 400 nm).